












TECH BRIEFS

NATIONAL AERONAUTICS AND SPACE ADMINISTRATION

-  **Technology Focus**
-  **Computers/Electronics**
-  **Software**
-  **Materials**
-  **Mechanics**
-  **Machinery/Automation**
-  **Manufacturing**
-  **Bio-Medical**
-  **Physical Sciences**
-  **Information Sciences**
-  **Books and Reports**

INTRODUCTION

Tech Briefs are short announcements of innovations originating from research and development activities of the National Aeronautics and Space Administration. They emphasize information considered likely to be transferable across industrial, regional, or disciplinary lines and are issued to encourage commercial application.

Availability of NASA Tech Briefs and TSPs

Requests for individual Tech Briefs or for Technical Support Packages (TSPs) announced herein should be addressed to

National Technology Transfer Center

Telephone No. (800) 678-6882 or via World Wide Web at www2.nttc.edu/leads/

Please reference the control numbers appearing at the end of each Tech Brief. Information on NASA's Commercial Technology Team, its documents, and services is also available at the same facility or on the World Wide Web at www.nctn.hq.nasa.gov.

Innovative Partnerships Offices are located at NASA field centers to provide technology-transfer access to industrial users. Inquiries can be made by contacting NASA field centers and Mission Directorates listed below.

NASA Field Centers and Program Offices

Ames Research Center

Lisa L. Lockyer
(650) 604-1754
lisa.l.lockyer@nasa.gov

Dryden Flight Research Center

Gregory Poteat
(661) 276-3872
greg.poteat@dfrc.nasa.gov

Goddard Space Flight Center

Nona Cheeks
(301) 286-5810
Nona.K.Cheeks.1@nasa.gov

Jet Propulsion Laboratory

Ken Wolfenbarger
(818) 354-3821
james.k.wolfenbarger@jpl.nasa.gov

Johnson Space Center

Helen Lane
(713) 483-7165
helen.w.lane@nasa.gov

Kennedy Space Center

Jim Aliberti
(321) 867-6224
Jim.Aliberti-1@nasa.gov

Langley Research Center

Ray P. Turcotte
(757) 864-8881
r.p.turcotte@larc.nasa.gov

John H. Glenn Research Center at Lewis Field

Robert Lawrence
(216) 433-2921
robert.f.lawrence@nasa.gov

Marshall Space Flight Center

Vernotto McMillan
(256) 544-2615
vernotto.mcmillan@msfc.nasa.gov

Stennis Space Center

John Bailey
(228) 688-1660
john.w.bailey@nasa.gov

NASA Mission Directorates

At NASA Headquarters there are four Mission Directorates under which there are seven major program offices that develop and oversee technology projects of potential interest to industry:

Carl Ray

Small Business Innovation Research Program (SBIR) & Small Business Technology Transfer Program (STTR)
(202) 358-4652
carl.g.ray@nasa.gov

Frank Schowengerdt

Innovative Partnerships Program (Code TD)
(202) 358-2560
fschowen@hq.nasa.gov

John Mankins

Exploration Systems Research and Technology Division
(202) 358-4659
john.c.mankins@nasa.gov

Terry Hertz

Aeronautics and Space Mission Directorate
(202) 358-4636
thertz@mail.hq.nasa.gov

Glen Mucklow

Mission and Systems Management Division (SMD)
(202) 358-2235
gmucklow@mail.hq.nasa.gov

Granville Paules

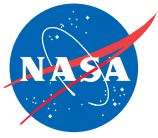
Mission and Systems Management Division (SMD)
(202) 358-0706
gpaules@mtpe.hq.nasa.gov

Gene Trinh

Human Systems Research and Technology Division (ESMD)
(202) 358-1490
eugene.h.trinh@nasa.gov

John Rush

Space Communications Office (SOMD)
(202) 358-4819
john.j.rush@nasa.gov



TECH BRIEFS

NATIONAL AERONAUTICS AND SPACE ADMINISTRATION



5 Thin-Film Resistance Heat-Flux Sensors

- 5 Thin-Film Resistance Heat-Flux Sensors
- 6 Circuit Indicates That Voice-Recording Disks Are Nearly Full
- 7 Optical Sensing of Combustion Instabilities in Gas Turbines
- 7 Crane-Load Contact Sensor



9 Electronics/Computers

- 9 Hexagonal and Pentagonal Fractal Multiband Antennas
- 10 Multifunctional Logic Gate Controlled by Temperature
- 11 Multifunctional Logic Gate Controlled by Supply Voltage
- 12 Power Divider for Waveforms Rich in Harmonics
- 12 SCB Quantum Computers Using iSWAP and 1-Qubit Rotations



15 Software

- 15 CSAM Metrology Software Tool
- 15 Update on Rover Sequencing and Visualization Program
- 15 Selecting Data From a Star Catalog



17 Mechanics

- 17 Rotating Desk for Collaboration by Two Computer Programmers
- 18 Variable-Pressure Washer



19 Machinery/Automation

- 19 Magnetically Attached Multifunction Maintenance Rover



21 Manufacturing

- 21 Improvements in Fabrication of Sand/Binder Cores for Casting
- 22 Solid Freeform Fabrication of Composite-Material Objects



25 Physical Sciences

- 25 Efficient Computational Model of Hysteresis
- 26 Gauges for Highly Precise Metrology of a Compound Mirror
- 27 Improved Electrolytic Hydrogen Peroxide Generator
- 27 High-Power Fiber Lasers Using Photonic Band Gap Materials



29 Information Sciences

- 29 Ontology-Driven Information Integration



31 Books & Reports

- 31 Quantifying Traversability of Terrain for a Mobile Robot
- 31 More About Arc-Welding Process for Making Carbon Nanotubes
- 31 Controlling Laser Spot Size in Outer Space
- 31 Software-Reconfigurable Processors for Spacecraft

This document was prepared under the sponsorship of the National Aeronautics and Space Administration. Neither the United States Government nor any person acting on behalf of the United States Government assumes any liability resulting from the use of the information contained in this document, or warrants that such use will be free from privately owned rights.



Thin-Film Resistance Heat-Flux Sensors

Comparative advantages would be larger output signals and greater ease of fabrication.

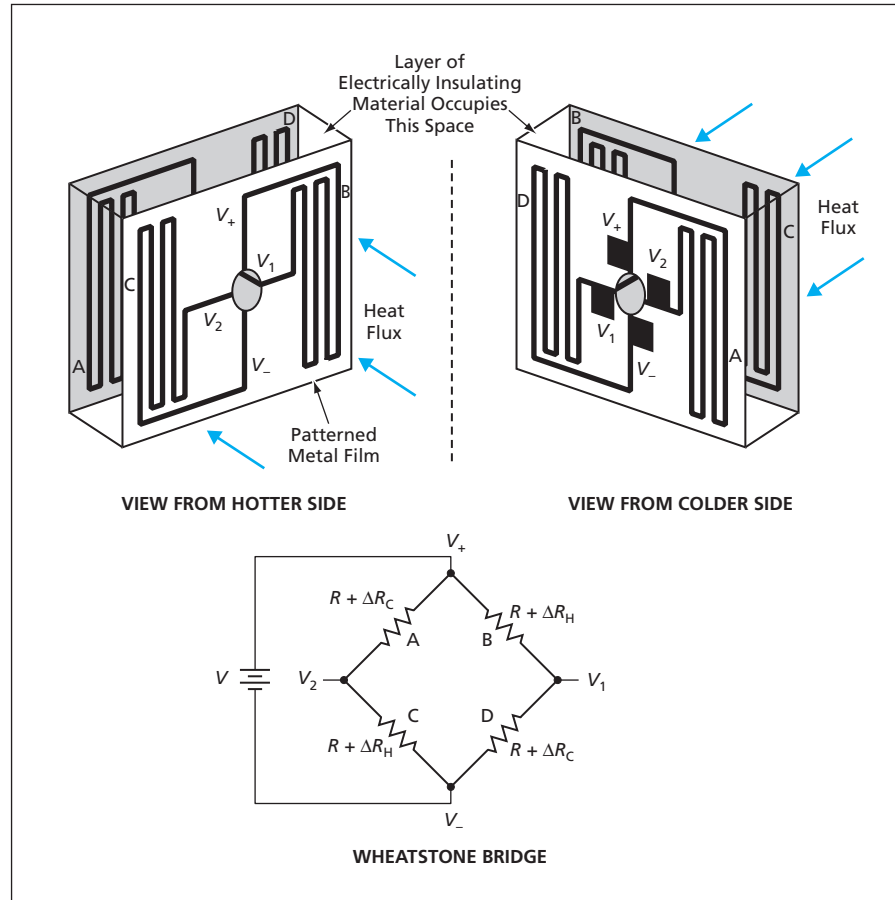
John H. Glenn Research Center, Cleveland, Ohio

Thin-film heat-flux sensors of a proposed type would offer advantages over currently available thin-film heat flux sensors. Like a currently available thin-film heat-flux sensor, a sensor according to the proposal would be based on measurement of voltages related to the temperatures of thin metal films on the hotter and colder faces of a layer of an electrically insulating and moderately thermally conductive material. The heat flux through such a device is proportional to the difference between the temperatures and to the thermal conductivity of the layer. The advantages of the proposed sensors over the commercial ones would arise from the manner in which the temperature-related voltages would be generated and measured.

In currently available thin-film heat-flux sensors, the temperature-related voltages are generated by thin-film thermocouples. The voltages generated by the thermocouples are small, making it difficult to operate the sensors. Moreover, fabrication and calibration of the commercial sensors are made difficult by the basic nature of their designs, which call for precise deposition of layers of multiple materials to form the thermocouples.

A sensor according to the proposal would not exploit the thermocouple principle to generate the temperature-related voltages. Instead, it would exploit the temperature dependence of the electrical resistivity of a single metal, which would be deposited in the form of patterned thin films on opposite sides of a layer of electrically insulating and moderately thermally conductive material. The use of a single metal, as opposed to at least two metals for a thermocouple, would make fabrication easier. The single-metal design would also make it feasible to fabricate sensors in batches.

The basic principle of design and operation of the proposed sensors admits of wide variations in sizes, shapes, and materials to suit specific applications. Common to all designs is that the films would be patterned to form arms of Wheatstone bridges with contact pads for connection to external measurement



Thin Metal Films Would Be Patterned on opposite faces of a layer of electrically insulating material as arms of a Wheatstone bridge. The output of the bridge would be proportional to the difference in electrical resistance approximately proportional to a difference in temperature across the layer.

circuitry. In every design (see figure), the metal films would be patterned so that two arms of the Wheatstone bridge would be on the hotter side (arms B and C) and two arms would be on the colder side (arms A and D). An excitatory potential, $V = V_+ - V_-$, would be applied to the bridge. The response of the bridge due to the heat flux would be given by

$$\Delta V = V_2 - V_1 = V \frac{\Delta R_H - \Delta R_C}{2R + \Delta R_H + \Delta R_C}$$

where V_1 and V_2 are the potentials at the points so labeled in the figure, R is the electrical resistance of the bridge in the absence of any temperature difference or heat flux, and ΔR_H is the change in resistance of legs B and C on the hot side

and ΔR_C is the change in resistance of legs A and D on the cold side. For a given temperature difference, the ΔV generated by this sensor would be an order of magnitude greater than the voltage generated by a thermocouple-based sensor.

This work was done by Gustave C. Fralick and John D. Wrbanek of Glenn Research Center and Charles A. Blaha of Akima Corp. Further information is contained in a TSP (see page 1).

Inquiries concerning rights for the commercial use of this invention should be addressed to NASA Glenn Research Center, Innovative Partnerships Office, Attn: Steve Fedor, Mail Stop 4-8, 21000 Brookpark Road, Cleveland, Ohio 44135. Refer to LEW-17306-1.

Circuit Indicates That Voice-Recording Disks Are Nearly Full

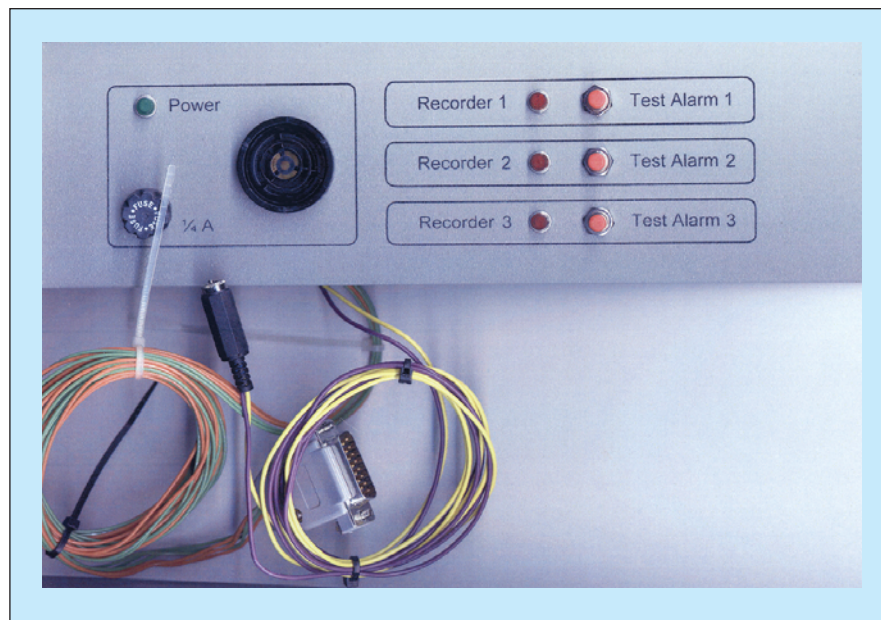
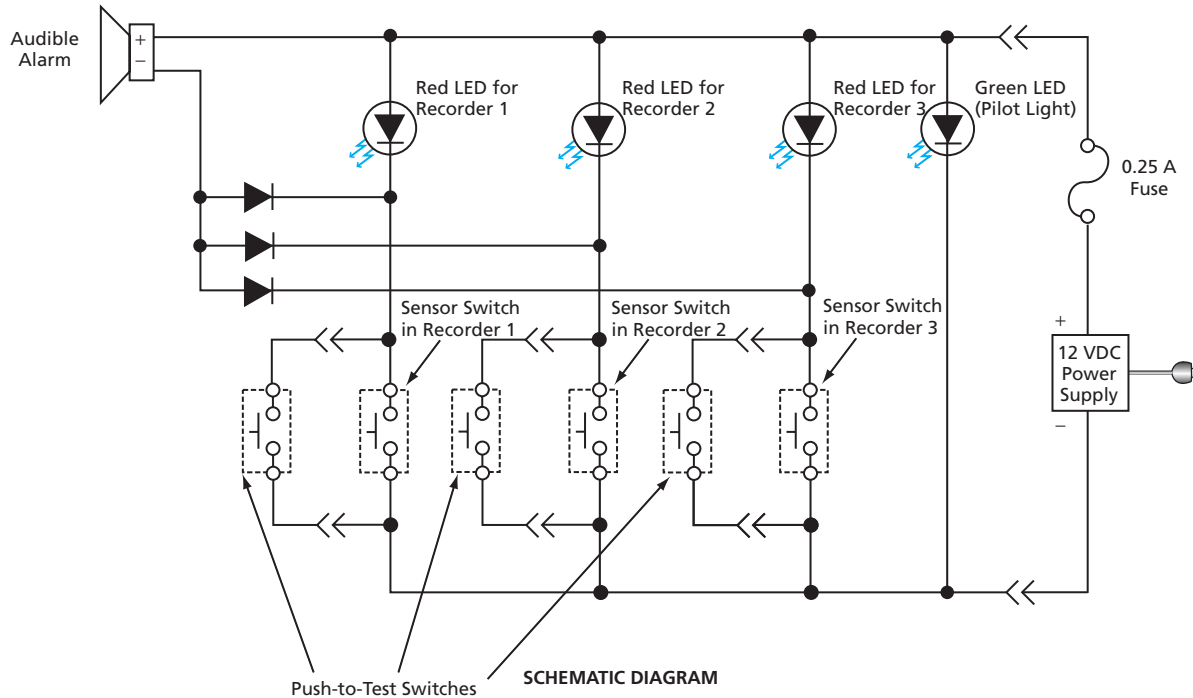
Visible and audible alarm signals summon technicians to change recording disks.

NASA's Jet Propulsion Laboratory, Pasadena, California

A remote alarm circuit provides visible and audible signals to indicate that there is little unused space left on magnetic and optical tracks on disks used to record voice signals in a group of

three multichannel voice recorders. In the particular application for which the remote alarm circuit was built, the voice recorders are required to operate without interruption, but the techni-

cians responsible for the continuous operation of the voice recorders perform most of their duties on a different floor of the building in which the voice recorders are located. The remote



PHOTOGRAPHY OF FRONT PANEL

An Audible Alarm and LED Indicators signal when remote voice recorders are low on available recording media space. A pilot LED and push-to-test buttons enable periodic verification of the alarm panel without interfering with alarm functions.

alarm circuit gives sufficient advance warning to enable the technicians to go to the voice recorders and change recording disks in time to ensure continuity of recording.

The circuit (see figure) includes a sensor in each voice recorder that closes a switch when the unused space on the recording disk falls below a preset minimum. A sensor switch closure indicates a fault condition in which an audible alarm activates together with a light-emitting diode (LED) for the corresponding fault. Three current steer-

ing diodes make the voltage across, and current through, the audible alarm independent from the number of simultaneous faults. This keeps the alarm tone consistent despite the number of alarms.

For verifying the alarm panel, normally-open push-button switches are wired in parallel with the remote sensor switches. This arrangement decouples the test circuitry from the alarm circuitry, which (1) allows each alarm to be tested without the presence of a fault condition on a voice

recorder, and (2) prevents any failure in the test circuitry itself from disabling an alarm indication when an actual fault condition is present on a voice recorder. Pressing a push-to-test button causes the audible alarm to signal and the corresponding voice recorder LED to light. A green LED is used as a pilot light.

This work was done by Harold Minuskin of NASA's Jet Propulsion Laboratory and by John Pastor of XteQ, Inc. Further information is contained in a TSP (see page 1). NPO-40150

Optical Sensing of Combustion Instabilities in Gas Turbines Engine operation is diagnosed via infrared radiation emitted by exhaust gases.

John H. Glenn Research Center, Cleveland, Ohio

In a continuing program of research and development, a system has been demonstrated that makes high-speed measurements of thermal infrared radiance from gas-turbine engine exhaust streams. When a gas-turbine engine is operated under conditions that minimize the emission of pollutants, there is a risk of crossing the boundary from stable to unstable combustion. Combustion instability can lead to engine damage and even catastrophic failure. Sensor systems of the type under development could provide valuable data during the development testing of gas-turbine engines or of engine components.

A system of the type under development makes high-speed measurements of thermal infrared radiance from the engine exhaust stream. The sensors of this system can be mounted outside the

engine, which eliminates the need for engine case penetrations typical with other engine dynamics monitors. This is an important advantage in that turbine-engine manufacturers consider such penetrations to be very undesirable.

A prototype infrared sensor system has been built and demonstrated on a turbine engine. This system includes rugged and inexpensive near-infrared sensors and filters that select wavelengths of infrared radiation for high sensitivity. In experiments, low-frequency signatures were consistently observed in the detector outputs. Under some conditions, the signatures also included frequency components having one or two radiance cycles per engine revolution. Although it has yet to be verified, it is thought that the low-frequency signatures may be associated

with bulk-mode combustion instabilities or flow instabilities in the compressor section of the engine, while the engine-revolution-related signatures may be indicative of mechanical problems in the engine. The system also demonstrated the ability to detect transient high-radiance events. These events indicate hot spots in the exhaust stream and were found to increase in frequency during engine acceleration.

This work was done by James R. Markham, David F. Marran, and James J. Scire, Jr., of Advanced Fuel Research, Inc., for Glenn Research Center.

Inquiries concerning rights for the commercial use of this invention should be addressed to NASA Glenn Research Center, Innovative Partnerships Office, Attn: Steve Fedor, Mail Stop 4-8, 21000 Brookpark Road, Cleveland, Ohio 44135. Refer to LEW-17355.

Crane-Load Contact Sensor

The decrease in electrical impedance upon contact is used to detect contact.

John F. Kennedy Space Center, Florida

An electronic instrument has been developed as a prototype of a portable crane-load contact sensor. Such a sensor could be helpful in an application in which the load rests on a base in a horizontal position determined by vertical alignment pins (see Figure 1). If the crane is not positioned to lift the load precisely vertically, then the load can be expected to swing once it has been lifted clear of the pins. If the load is especially heavy, large, and/or fragile, it

could hurt workers and/or damage itself and nearby objects. By indicating whether the load remains in contact with the pins when it has been lifted a fraction of the length of the pins, the crane-load contact sensor helps the crane operator determine whether it is safe to lift the load clear of the pins: If there is contact, then the load is resting against the sides of the pins and, hence, it may not be safe to lift; if contact is occasionally broken, then the load is prob-

ably not resting against the pins, so it should be safe to lift.

It is assumed that the load and base, or at least the pins and the surfaces of the alignment holes in the load, are electrically conductive, so the instrument can use electrical contact to indicate mechanical contact. However, DC resistance cannot be used as an indicator of contact for the following reasons: The load and the base are both electrically grounded

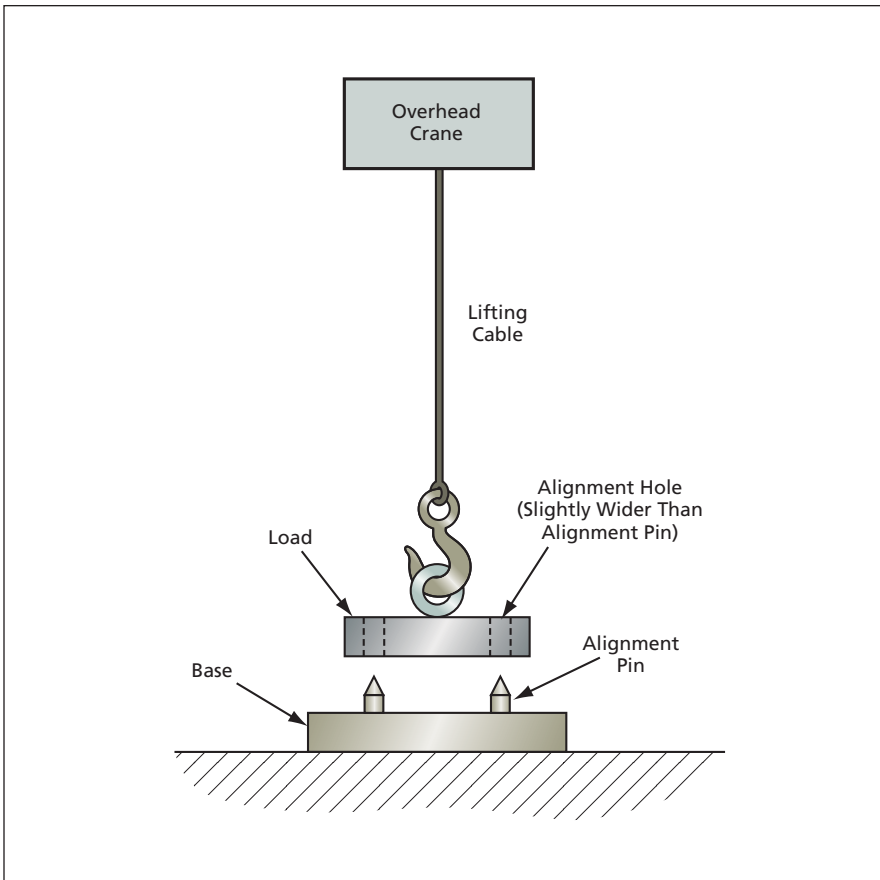


Figure 1. The **Load Must Be Lifted** precisely vertically, or else it will swing when it clears the alignment pins. This means that the crane must be positioned so that during initial lifting, the load does not press sideways against the pins.

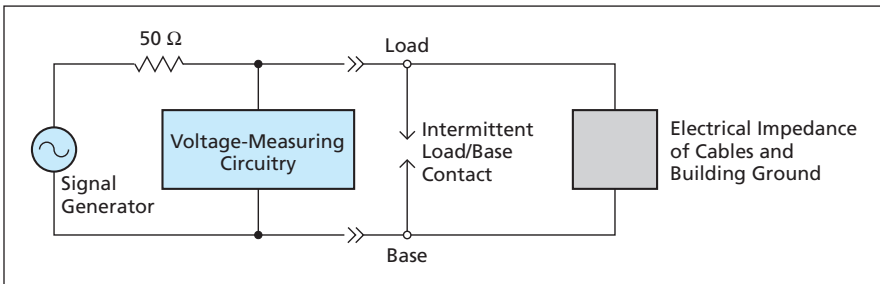


Figure 2. The **Crane-Load Contact Sensor**, shown here greatly simplified for the sake of clarity, measures a voltage related to the base-to-load electrical impedance to determine whether the load and pins are in contact.

through cables (the load is grounded through the lifting cable of the crane) to prevent discharge of static electricity. In other words, the DC resistance between the load and the pins is always low, as though they were always in direct contact.

Therefore, instead of DC resistance, the instrument utilizes the AC electrical impedance between the pins and the load. The signal frequency used in the measurement is high enough (≈ 1 MHz) that the impedance contributed by the cables and the electrical ground network of the building in which the crane and the base are situated is significantly greater than the contact impedance between the pins and the load.

The instrument includes a signal generator and voltage-measuring circuitry, and is connected to the load and the base as shown in Figure 2. The output of the signal generator (typically having amplitude of the order of a volt) is applied to the load via a 50- Ω resistor, and the voltage between the load and the pins is measured. When the load and the pins are not in contact, the impedance between them is relatively high, causing the measured voltage to exceed a threshold value. When the load and the pins are in contact, the impedance between them falls to a much lower value, causing the voltage to fall below the threshold value. The voltage-measuring circuitry turns on a red light-emitting diode (LED) to indicate the lower-voltage/contact condition. Whenever the contact has been broken and the non-contact/higher-voltage condition has lasted for more than 2 ms, the voltage-measuring circuitry indicates this condition by blinking a green LED.

This work was done by Robert Youngquist of Kennedy Space Center and Carlos Mata and Robert Cox of ASRC Aerospace. Further information is contained in a TSP (see page 1). KSC-12702



Hexagonal and Pentagonal Fractal Multiband Antennas

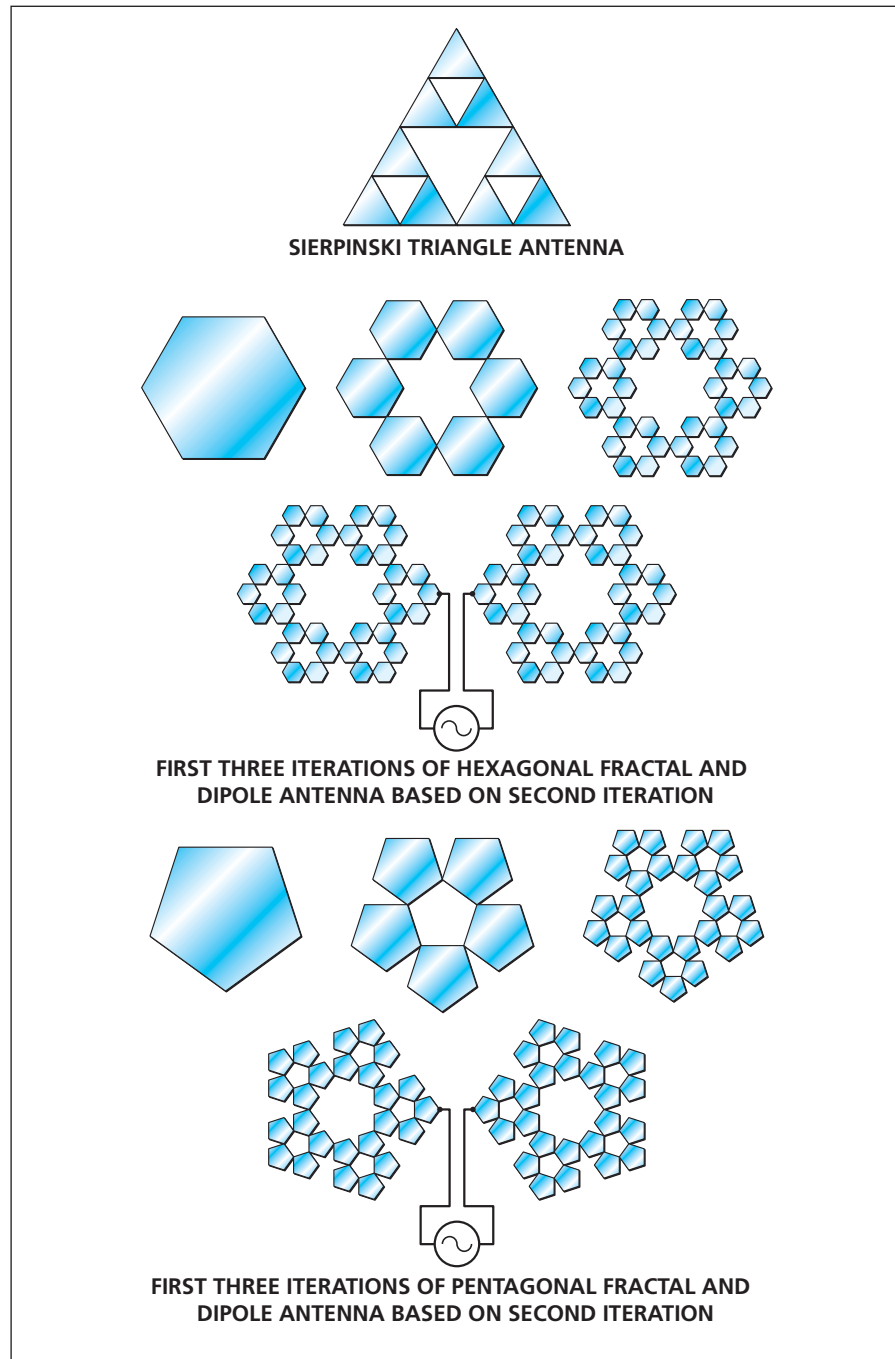
These antennas could be suitable for multifunctional wireless-communication products.

John F. Kennedy Space Center, Florida

Multiband dipole antennas based on hexagonal and pentagonal fractals have been analyzed by computational simulations and functionally demonstrated in experiments on prototypes. These antennas are capable of multiband or wide-band operation because they are subdivided into progressively smaller substructures that resonate at progressively higher frequencies by virtue of their smaller dimensions. The novelty of the present antennas lies in their specific hexagonal and pentagonal fractal configurations and the resonant frequencies associated with them. These antennas are potentially applicable to a variety of multiband and wide-band commercial wireless-communication products operating at different frequencies, including personal digital assistants, cellular telephones, pagers, satellite radios, Global Positioning System receivers, and products that combine two or more of the aforementioned functions.

Perhaps the best-known prior multiband antenna based on fractal geometry is the Sierpinski triangle antenna (also known as the Sierpinski gasket), shown in the top part of the figure. In this antenna, the scale length at each iteration of the fractal is half the scale length of the preceding iteration, yielding successive resonant frequencies related by a ratio of about 2. The middle and bottom parts of the figure depict the first three iterations of the hexagonal and pentagonal fractals along with typical dipole-antenna configuration based on the second iteration. Successive resonant frequencies of the hexagonal fractal antenna have been found to be related by a ratio of about 3, and those of the pentagonal fractal antenna by a ratio of about 2.59.

This work was done by Philip W. Tang of Kennedy Space Center and Parveen Wahid of the University of Central Florida. Further information is contained in a TSP (see page 1). KSC-12393/482



Hexagonal and Pentagonal Fractal Antennas complement the Sierpinski triangle antenna as options for design of multiband and wide-band wireless-communication products.

Multifunctional Logic Gate Controlled by Temperature

This circuit performs different logic functions at different temperatures.

NASA's Jet Propulsion Laboratory, Pasadena, California

The figure is a schematic diagram of a complementary metal oxide/semiconductor (CMOS) electronic circuit that has been designed to function as a NAND gate at a temperature between 0 and 80 °C and as a NOR gate at temperatures from 120 to 200 °C. In the intermediate temperature range of 80 to 120 °C, this circuit is expected to perform a function intermediate between NAND and NOR with degraded noise margin. The process of designing the circuit and the planned fabrication and testing of the circuit are parts of demonstration of polymorphic electronics — a technological discipline that emphasizes designing the same circuit to perform different analog and/or digital functions under different conditions. In this case, the different conditions are different temperatures.

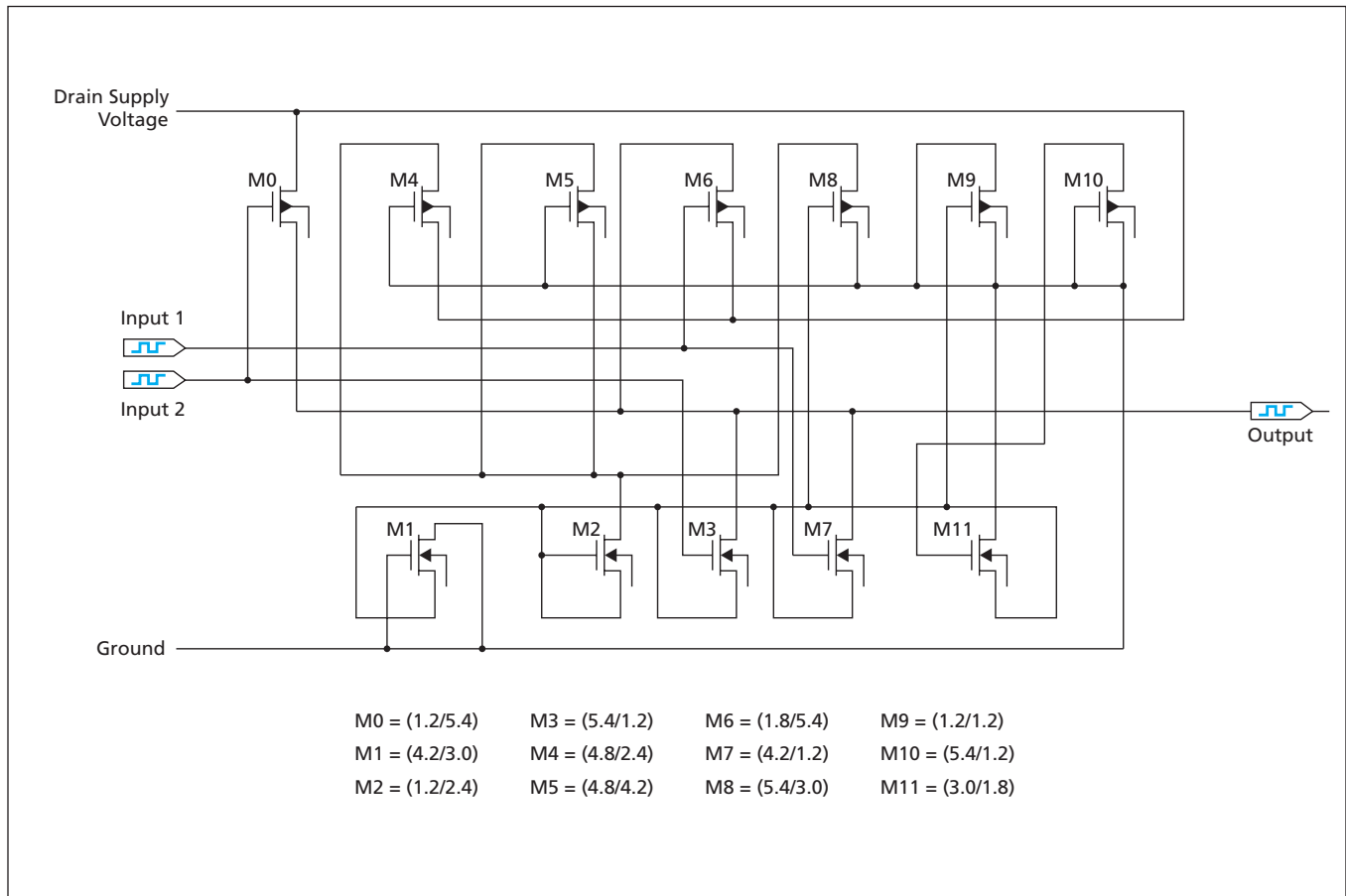
A more extensive discussion of polymorphic electronics was presented in "Polymorphic Electronic Circuits" (NPO-

21213), *NASA Tech Briefs*, Vol. 28, No. 4 (April 2004), page 38. To recapitulate: The traditional approach to design is abandoned in favor of an evolutionary approach to impart the desired multiple functionality to a circuit. In the evolutionary approach, one designs, constructs, and tests a sequence of populations of circuits that function as incrementally better solutions of a given design problem through the selective, repetitive connection and/or disconnection of capacitors, transistors, amplifiers, inverters, and/or other circuit building blocks. The evolution is guided by a search-and-optimization algorithm (in particular, a genetic algorithm) that operates in the space of possible circuits to find a circuit that exhibits an acceptably close approximation of the desired functionality.

In the evolutionary approach, a circuit design can be tested by computational simulation, tested in real hardware, or tested in random sequences of computational

simulation and real hardware. In the present case, the designed functionality has been tested thus far by computational simulation and also in real time. The computational simulations have included many tests to assess the robustness of the NAND and NOR gate performances in the presence of noise, for all possible sequences of positive and negative input-signal transitions, and under changes in diverse parameters that include not only temperature but also switching speed, power dissipation, power-supply voltage, transistor sizes, and changes in the transistor model between two commercial fabrication processes. These tests showed the performances to be robust, and once fabricated, the circuit performed as intended.

This work was done by Adrian Stoica and Ricardo Zebulum of Caltech for NASA's Jet Propulsion Laboratory. Further information is contained in a TSP (see page 1). NPO-30795



This Circuit Performs as One of Two Logic Gates, depending on the temperature. Between 0 and 80 °C, it is a NAND gate; between 120 and 200 °C, it is a NOR gate. The labels M0 through M11 refer to twelve transistors in this circuit. The first and second numbers in parentheses next to each label are the width and length, respectively, of the transistor in microns.

Multifunctional Logic Gate Controlled by Supply Voltage

This circuit performs different logic functions at different levels of supply voltage.

NASA's Jet Propulsion Laboratory, Pasadena, California

The figure is a schematic diagram of a complementary metal oxide/semiconductor (CMOS) electronic circuit that functions as a NAND gate at a power-supply potential (V_{dd}) of 3.3 V and as NOR gate for $V_{dd} = 1.8$ V. In the intermediate V_{dd} range of 1.8 to 3.3 V, this circuit performs a function intermediate between NAND and NOR with degraded noise margin. Like the circuit of the immediately preceding article, this circuit serves as a demonstration of the evolutionary approach to design of polymorphic electronics — a technological discipline that emphasizes evolution of the design of a circuit to perform different analog and/or digital functions under different conditions. In this instance, the different conditions are different values of V_{dd} .

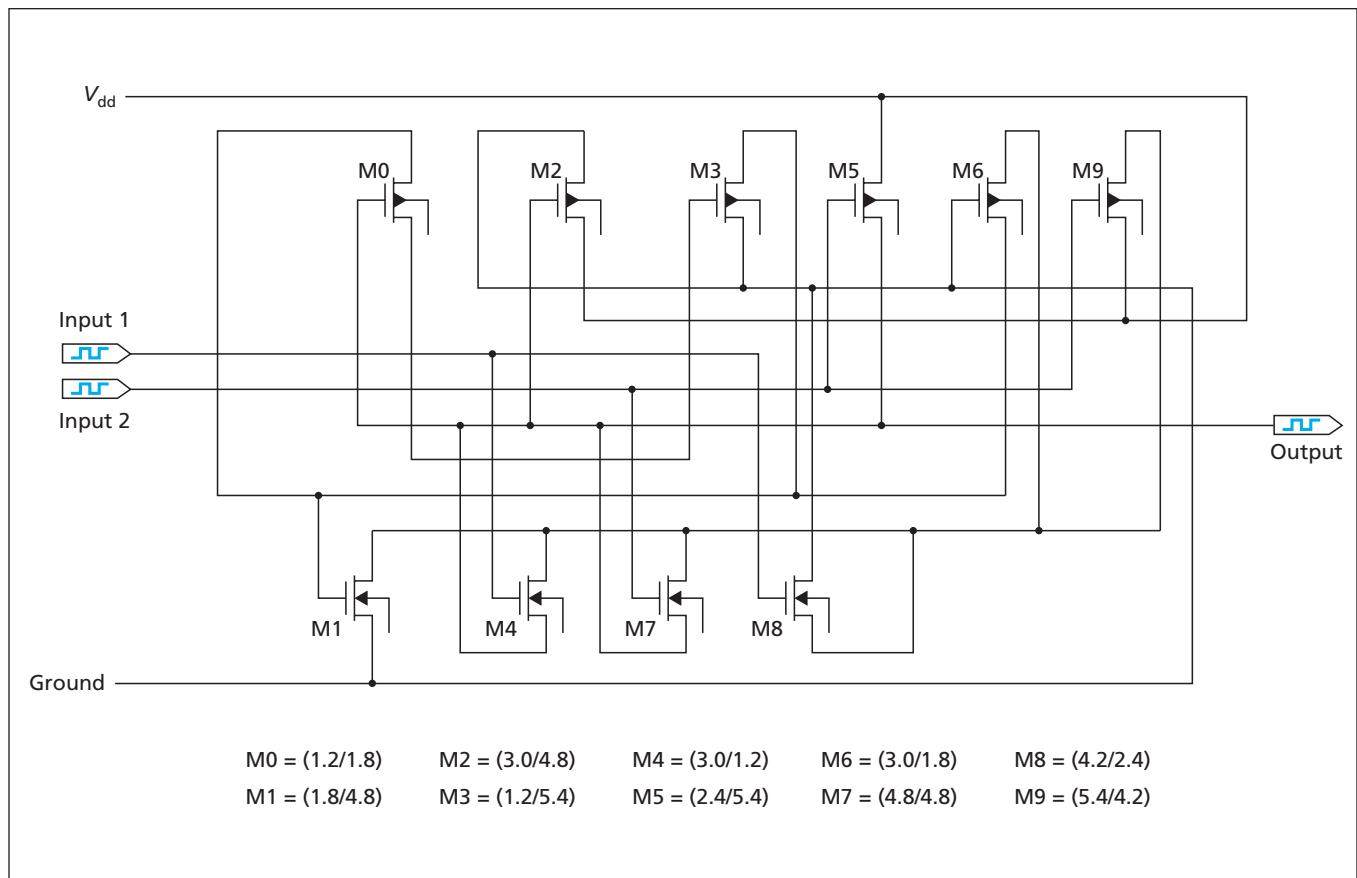
This demonstration is a step toward the development of a variety of logic gates, the functionalities of which can

be changed by a single global signal — in this case, V_{dd} . The state-of-the-art logic circuits with which polymorphic logic circuits can be expected to compete are the configurable logic blocks (CLBs) of field-programmable gate arrays (FPGAs). The reconfiguration of a typical CLB involves multiplexing, switching, and downloading of thousands of bits from a lookup-table memory circuit. To configure in excess of thousands of CLBs in a larger FPGA may take even seconds; moreover, for satellite/spacecraft FPGA for which a new configuration is sent from Earth through a slow uplink communication, the time to reconfigure could be much longer. The main advantages of the type of polymorphism demonstrated here are the rapidity of the change in functionality and the simplicity of the circuitry needed to effect the change: Simply by changing V_{dd} , the functionalities of thousands of

logic cells can be changed within nanoseconds, without multiplexing and without switches or lookup tables.

As in the case of the preceding article, the functionality of the present circuit has been tested by computational simulations. The simulations have tested the robustness of the circuit in the presence of input noise, for all possible sequences of positive and negative input-signal transitions, and under changes in parameters that include not only V_{dd} but, also temperature, switching speed, fan-out, and power dissipation. In addition, the circuit has been fabricated on a silicon chip and verified to function substantially as intended. This is the first circuit designed by artificial evolution to be so realized.

This work was done by Adrian Stoica and Ricardo Zebulum of Caltech for NASA's Jet Propulsion Laboratory. Further information is contained in a TSP (see page 1). NPO-30836



This Circuit Performs as One of Two Logic Gates, depending on V_{dd} . At $V_{dd} = 3.3$ V, it is a NAND gate; at $V_{dd} = 1.8$ V, it is a NOR gate. The labels M0 through M9 refer to 10 CMOS transistors in this circuit. The first and second numbers in parentheses next to each label are the width and length, respectively, of the transistor in microns.

Power Divider for Waveforms Rich in Harmonics

The power of a square-wave signal can be divided without adverse effect on either the amplitude or phase of the waveform.

Marshall Space Flight Center, Alabama

A method for dividing the power of an electronic signal rich in harmonics involves the use of an improved divider topology. A divider designed with this topology could be used, for example, to propagate a square-wave signal in an amplifier designed with a push-pull configuration

to enable the generation of more power than could be generated in another configuration.

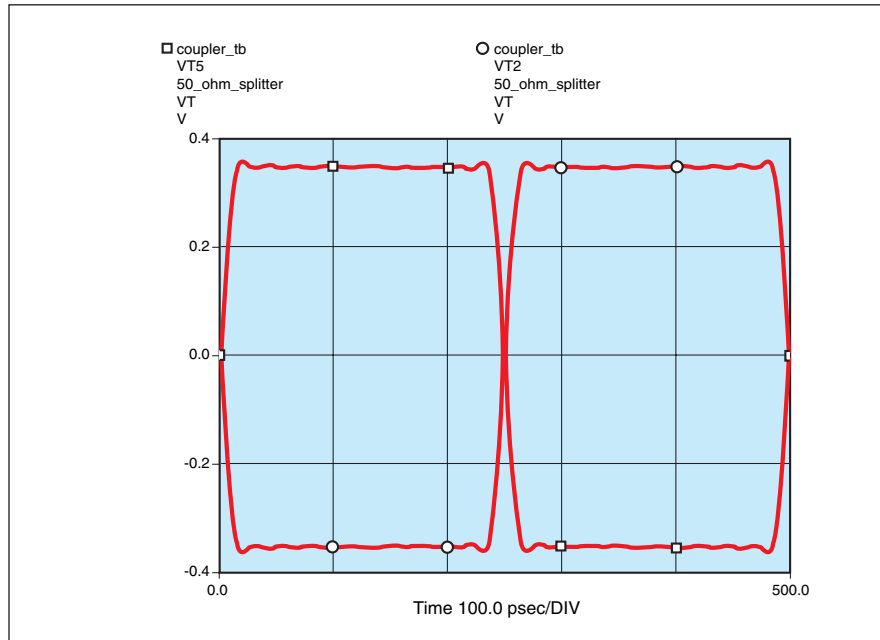
Many power-divider topologies have been conceived for application in power amplifiers operating at microwave and lower radio frequencies. Some examples

are (1) the Wilkinson hybrid topology, which is restricted to division by powers of two, (2) the radial-wave power hybrid topology, which includes a lumped-element filter network, and (3) the circular-sector topology, which features a narrow usable frequency range.

The present improved topology was developed for an application in which there is a requirement to divide the power of a square-wave radio signal and deliver the signal to an antenna. Another requirement is to maintain the relative-amplitude and phase relationship between the fundamental-frequency component and each of the harmonic-frequency components. The present improved power-divider topology satisfies these requirements. The figure presents an example of output waveforms from a power divider of this topology.

This work was done by William Herbert Sims III of Marshall Space Flight Center. Further information is contained in a TSP (see page 1).

This invention has been patented by NASA (U.S. Patent No. 6,320,478). Inquiries concerning nonexclusive or exclusive license for its commercial development should be addressed to Sammy Nabors, MSFC Commercialization Assistance Lead, at (256) 544-5226 or sammy.a.nabors@nasa.gov. Refer to MFS-31186.



These Two Waveforms at Output Ports of a 50- Ω Power Divider are 180° out of phase with each other and resemble the input waveform.

SCB Quantum Computers Using iSWAP and 1-Qubit Rotations

Practical implementation in the SCB context appears to be feasible.

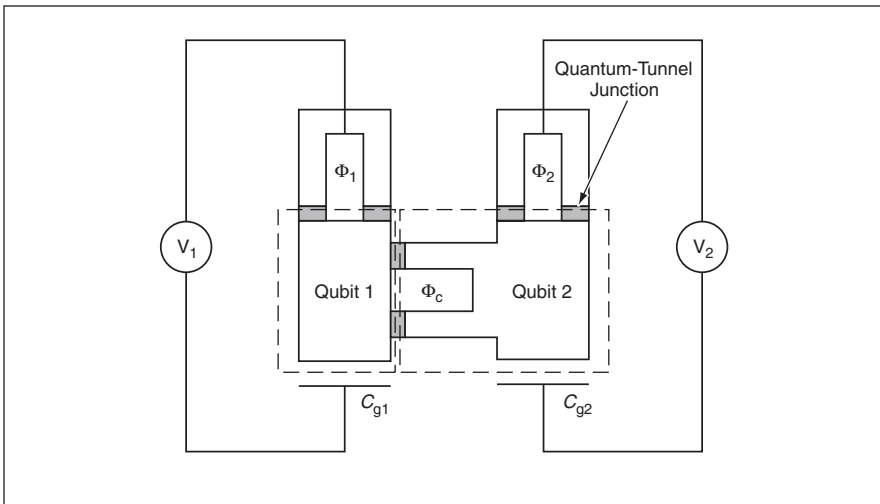
NASA's Jet Propulsion Laboratory, Pasadena, California

Units of superconducting circuitry that exploit the concept of the single-Cooper-pair box (SCB) have been built and are undergoing testing as prototypes of logic gates that could, in principle, constitute building blocks of clocked quantum computers. These units utilize quantized charge states as the quantum information-bearing degrees of freedom.

An SCB is an artificial two-level quantum system that comprises a nanoscale superconducting electrode connected to a reservoir of Cooper-pair charges via a Josephson junction. The logical quantum states of the device, $|0\rangle$ and $|1\rangle$, are

implemented physically as a pair of charge-number states that differ by $2e$ (where e is the charge of an electron). Typically, some 10^9 Cooper pairs are involved. Transitions between the logical states are accomplished by tunneling of Cooper pairs through the Josephson junction. Although the two-level system contains a macroscopic number of charges, in the superconducting regime, they behave collectively, as a Bose-Einstein condensate, making possible a coherent superposition of the two logical states. This possibility makes the SCB a candidate for the physical implementation of a qubit.

A set of quantum logic operations and the gates that implement them is characterized as universal if, in principle, one can form combinations of the operations in the set to implement any desired quantum computation. To be able to design a practical quantum computer, one must first specify how to decompose any valid quantum computation into a sequence of elementary 1- and 2-qubit quantum gates that are universal and that can be realized in hardware that is feasible to fabricate. Traditionally, the set of universal gates has been taken to be the set of all 1-qubit quantum gates in conjunction with the



In this **Two-Qubit Quantum Gate**, two qubits are coupled by use of two tunnel junctions connected in parallel. This design makes it possible to turn the coupling on or off as necessary. The Φ symbols represent applied magnetic fluxes, the C symbols denote coupling capacitances, and the V symbols denote voltage-measuring circuits and the corresponding measured voltages.

controlled-NOT (CNOT) gate, which is a 2-qubit gate. Also, it has been known for some time that the SWAP gate, which implements square root of the simple 2-qubit exchange interaction, is as computationally universal as is the CNOT operation.

The present innovative SCB-based units are of two types: those that can implement any 1-qubit operation (phase shift and/or rotation) and those that can implement a recently discovered 2-qubit operation called

“complex SWAP” or “iSWAP.” The combination of these 1- and 2-qubit operations has been shown to be universal on the basis of the governing quantum-mechanical equations. The use of iSWAP instead of CNOT as the single 2-qubit primitive operation offers an advantage over the prior art in that in the SCB context, iSWAP can be implemented in hardware more easily. The figure schematically depicts a 2-qubit gate according to the present innovation.

Unlike in prior experimental quantum computer circuits, neither the starting time nor the duration of a gate operation is used as a control parameter to determine the nature of the operation. Instead, quantum gate operations are controlled by applying sequences of voltages and magnetic fluxes to single qubits or pairs of qubits: hence, quantum logic operations can be performed in predictable, fixed, time intervals; that is, they can be clocked. Hence, further, it is easier to integrate these units into large-scale circuits. The feasibility of fabricating such gates and large-scale quantum circuits by use of electron-beam lithography has been demonstrated.

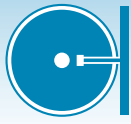
This work was done by Colin Williams and Pierre Echternach of Caltech for NASA's Jet Propulsion Laboratory. Further information is contained in a TSP (see page 1).

In accordance with Public Law 96-517, the contractor has elected to retain title to this invention. Inquiries concerning rights for its commercial use should be addressed to:

*Innovative Technology Assets Management
JPL*

*Mail Stop 202-233
4800 Oak Grove Drive
Pasadena, CA 91109-8099
(818) 354-2240*

*E-mail: iaoffice@jpl.nasa.gov
Refer to NPO-30213, volume and number of this NASA Tech Briefs issue, and the page number.*



CSAM Metrology Software Tool

CSAM Metrology Software Tool (CMeST) is a computer program for analysis of false-color CSAM images of plastic-encapsulated microcircuits. (“CSAM” signifies C-mode scanning acoustic microscopy.) The colors in the images indicate areas of delamination within the plastic packages. Heretofore, the images have been interpreted by human examiners. Hence, interpretations have not been entirely consistent and objective. CMeST processes the color information in image-data files to detect areas of delamination without incurring inconsistencies of subjective judgement. CMeST can be used to create a database of baseline images of packages acquired at given times for comparison with images of the same packages acquired at later times. Any area within an image can be selected for analysis, which can include examination of different delamination types by location. CMeST can also be used to perform statistical analyses of image data. Results of analyses are available in a spreadsheet format for further processing. The results can be exported to any data-base-processing software.

This program was written by Duc Vu, Michael Sandor, and Shri Agarwal of Caltech for NASA’s Jet Propulsion Laboratory. Further information is contained in a TSP (see page 1).

This software is available for commercial licensing. Please contact Karina Edmonds of the California Institute of Technology at (818) 393-2827. Refer to NPO-40475.

Update on Rover Sequencing and Visualization Program

The Rover Sequencing and Visualization Program (RSVP) has been updated. RSVP was reported in “Rover Sequencing and Visualization Program” (NPO-30845), *NASA Tech Briefs*, Vol. 29, No. 4 (April 2005), page 38. To recapitulate: The Rover Sequencing and Visualization Program (RSVP) is the software tool to be used in the Mars Exploration

Rover (MER) mission for planning rover operations and generating command sequences for accomplishing those operations. RSVP combines three-dimensional (3D) visualization for immersive exploration of the operations area, stereoscopic image display for high-resolution examination of the downlinked imagery, and a sophisticated command-sequence editing tool for analysis and completion of the sequences. RSVP is linked with actual flight code modules for operations rehearsal to provide feedback on the expected behavior of the rover prior to committing to a particular sequence. Playback tools allow for review of both rehearsed rover behavior and downlinked results of actual rover operations. These can be displayed simultaneously for comparison of rehearsed and actual activities for verification. The primary inputs to RSVP are downlink data products from the Operations Storage Server (OSS) and activity plans generated by the science team. The activity plans are high-level goals for the next day’s activities. The downlink data products include imagery, terrain models, and telemetered engineering data on rover activities and state. The Rover Sequence Editor (RoSE) component of RSVP performs activity expansion to command sequences, command creation and editing with setting of command parameters, and viewing and management of rover resources. The HyperDrive component of RSVP performs 2D and 3D visualization of the rover’s environment, graphical and animated review of rover predicted and telemetered state, and creation and editing of command sequences related to mobility and Instrument Deployment Device (robotic arm) operations. Additionally, RoSE and HyperDrive together evaluate command sequences for potential violations of flight and safety rules. The products of RSVP include command sequences for uplink that are stored in the Distributed Object Manager (DOM) and predicted rover state histories stored in the OSS for comparison and validation of downlinked telemetry. The majority of components comprising RSVP utilize the MER command and activity dictionaries to automatically customize the system for MER

activities. Thus, RSVP, being highly data driven, may be tailored to other missions with minimal effort. In addition, RSVP uses a distributed, message-passing architecture to allow multitasking and collaborative visualization and sequence development by scattered team members.

This tool was developed by Brian Cooper, Frank Hartman, Scott Maxwell, Jeng Yen, John Wright, and Carlos Balacuit of Caltech for NASA’s Jet Propulsion Laboratory. Further information is contained in a TSP (see page 1).

This software is available for commercial licensing. Please contact Karina Edmonds of the California Institute of Technology at (818) 393-2827. Refer to NPO-40353.

Selecting Data From a Star Catalog

MCDUMP is a computer program that selects data from the SKYMAP SKY2000 Master Star Catalog — a database about 150 MB in size, stored on a computer hard drive. The database describes about 300,000 stars, each by means of a 500-byte entry. MCDUMP reads all 300,000 entries, then generates an output file that comprises a subset of entries selected according to one or more criteria entered by the user. Examples of criteria that could be entered include: location in a selected portion of the sky; constancy or a specified degree of variability of brightness; absence of nearby, bright companion stars; a particular surface temperature; and brightness sufficient to enable detection by a specified astronomical instrument. The output of MCDUMP can be in the form of either a single 520-column file or multiple files that contain fewer columns to facilitate printing. MCDUMP has been configured and tested for use under the HP-UX 10.20 operating system (a Hewlett-Packard version of the UNIX operating system). It should also be possible to adapt MCDUMP to other versions of UNIX.

This program was written by David A. Tracewell of Goddard Space Flight Center and Christopher B. Sande of Computer Sciences Corporation. Further information is contained in a TSP (see page 1). GSC-14574



Rotating Desk for Collaboration by Two Computer Programmers

Two programmers can work together or alternately with minimal stress.

Goddard Space Flight Center, Greenbelt, Maryland

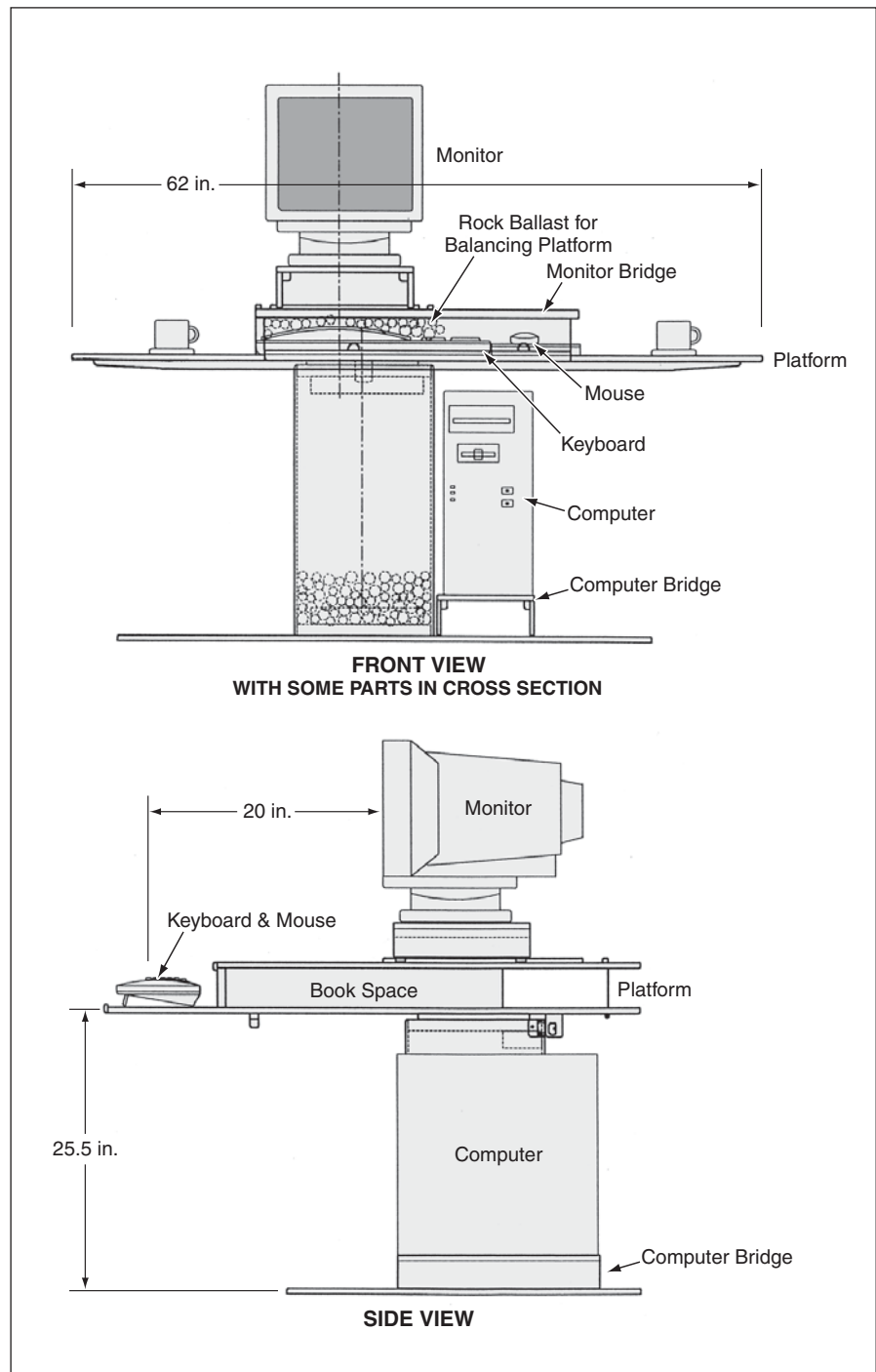
A special-purpose desk has been designed to facilitate collaboration by two computer programmers sharing one desktop computer or computer terminal. The impetus for the design is a trend toward what is known in the software industry as extreme programming — an approach intended to ensure high quality without sacrificing the quantity of computer code produced. Programmers working in pairs is a major feature of extreme programming.

The present desk design minimizes the stress of the collaborative work environment. It supports both quality and work flow by making it unnecessary for programmers to get in each other's way. The desk (see figure) includes a rotating platform that supports a computer video monitor, keyboard, and mouse. The desk enables one programmer to work on the keyboard for any amount of time and then the other programmer to take over without breaking the train of thought.

The rotating platform is supported by a turntable bearing that, in turn, is supported by a weighted base. The platform contains weights to improve its balance. The base includes a stand for a computer, and is shaped and dimensioned to provide adequate foot clearance for both users. The platform includes an adjustable stand for the monitor, a surface for the keyboard and mouse, and spaces for work papers, drinks, and snacks. The heights of the monitor, keyboard, and mouse are set to minimize stress.

The platform can be rotated through an angle of 40° to give either user a straight-on view of the monitor and full access to the keyboard and mouse. Magnetic latches keep the platform preferentially at either of the two extremes of rotation. To switch between users, one simply grabs the edge of the platform and pulls it around. The magnetic latch is easily released, allowing the platform to rotate freely to the position of the other user.

This work was done by John Thomas Riley for Goddard Space Flight Center. Further information is contained in a TSP (see page 1). GSC-14484



The Platform Rotates About a Vertical Axis through an angle of 40° to enable either of two programmers to use the keyboard and mouse and have a direct view of the monitor.

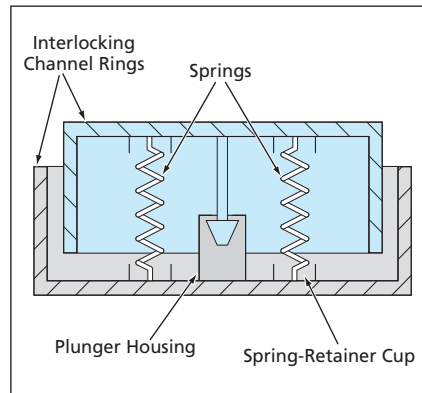
Variable-Pressure Washer

Clamping force would be applied in a specified nonuniform pattern.

Marshall Space Flight Center, Alabama

The variable-pressure washer (VPW) is a proposed device that is so named because (1) it would play the role similar to that played by an ordinary washer, except that (2) the clamping pressure applied by it would vary with either circumferential or radial position. In a typical contemplated application, the radially varying clamping pressure would be used to obtain more nearly uniform compression on a pair of concentric seals (e.g., an O-ring or a gasket) in an assembly that experiences larger deformations normal to the sealing surface for locations around the outer diameter of the attachment flange when compared to locations around the inner diameter.

The VPW (see figure) would include two interlocking channel rings pushed axially away from each other by compression springlike components located at two or more radial positions. Each spring would have a different stiffness based on the radial location. Overlap-



The Variable-Pressure Washer would contain springs of different stiffnesses at different locations about the central axis.

ping splits in each interlocking channel ring would allow for the non-uniform deformation in the rings. Each spring would be held in place by retaining cups attached to the inner flat surfaces of the channel rings. A plunger attached to one channel ring on the central axis

would be captured in a plunger housing attached to the other channel ring; The capture of the plunger would hold the VPW together.

When the VPW was clamped between two flat surfaces, the clamping force would be distributed unevenly across the face of the washer in the radial direction. The different stiffnesses of the springs would be chosen, in conjunction with other design parameters, to obtain a specified radial variation of clamping pressure in the presence of a specified clamping force.

This work was done by Stanley S. Smeltzer III and Z. Hector Estrada of Marshall Space Flight Center. For further information, contact Paul Hale at Paul.Hale@msfc.nasa.gov.

This invention is owned by NASA, and a patent application has been filed. For further information, contact Sammy Nabors, MSFC Commercialization Assistance Lead, at sammy.a.nabors@nasa.gov. Refer to MFS-31323

Magnetically Attached Multifunction Maintenance Rover

This robot could move along a ferromagnetic structure in any orientation.

NASA's Jet Propulsion Laboratory, Pasadena, California

A versatile mobile telerobot, denoted the magnetically attached multifunction maintenance rover (MAGMER), has been proposed for use in the inspection and maintenance of the surfaces of ships, tanks containing petrochemicals, and other large ferromagnetic struc-

tures. As its name suggests, this robot would utilize magnetic attraction to adhere to a structure. As it moved along the surface of the structure, the MAGMER would perform tasks that could include close-up visual inspection by use of video cameras, various sensors, and/or

and four pole pieces (see Figure 2). The wheels would protrude from between the pole pieces by only about 3 mm, so that the gap between the pole pieces and the ferromagnetic surface would be just large enough to permit motion along the surface but not so large as to reduce the magnetic attraction excessively. In addition to the wheel assemblies, the MAGMER would include magnetic adherence enhancement fixtures, which would comprise arrays of permanent magnets and pole pieces that could be adjusted to maximize or minimize the overall attractive magnetic force.

Even with a paint thickness of 2 mm, a preliminary design provides a safety factor of 5 in the magnetic force in the upside-down, water-jets-operating condition, in which the total load (including the weight of the MAGMER and cables and the water-jet force) would be about 260 lb (the weight of 118 kg). Optionally, the MAGMER could carry magnetic shielding and/or could be equipped with a demagnetizing module to remove residual magnetism from the structure.

The MAGMER would carry four charge-coupled-device cameras for visual inspection, monitoring of operation, navigation, and avoidance of collisions with obstacles. The control system of the MAGMER would include navigation and collision-avoidance subsystems that would utilize surface features as landmarks, in addition to direct images of obstacles.

This work was done by Yoseph Bar-Cohen and Benjamin Joffe of Caltech for NASA's Jet Propulsion Laboratory. Further information is contained in a TSP (see page 1).

In accordance with Public Law 96-517, the contractor has elected to retain title to this invention. Inquiries concerning rights for its commercial use should be addressed to:

*Innovative Technology Assets Management
JPL
Mail Stop 202-233
4800 Oak Grove Drive
Pasadena, CA 91109-8099
(818) 354-2240*

*E-mail: iaoffice@jpl.nasa.gov
Refer to NPO-20229, volume and number of this NASA Tech Briefs issue, and the page number.*

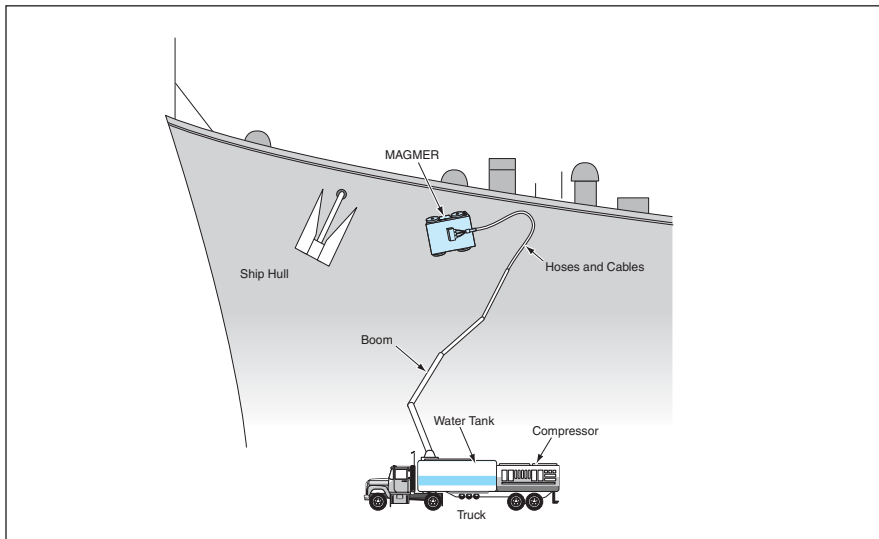


Figure 1. The MAGMER, Deployed From a Truck, would move along a ship hull surface. It would adhere to the hull by magnetic attraction.

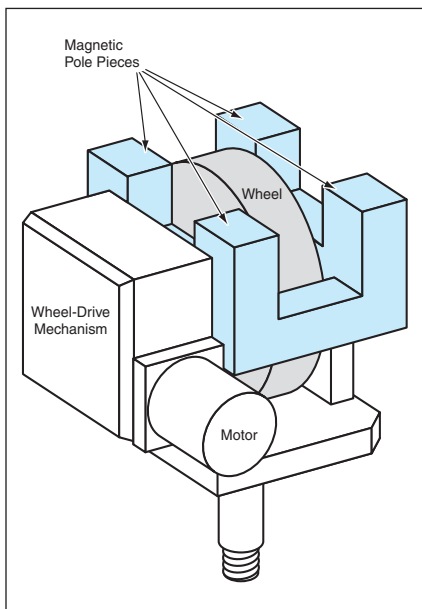


Figure 2. One of the Four Wheel Assemblies of the MAGMER is depicted here with the surface-adhering ends of the magnetic pole pieces facing upward.

removal of paint by water-jet blasting, laser heating, or induction heating.

The water-jet nozzles would be mounted coaxially within compressed-air-powered venturi nozzles that would collect the paint debris dislodged by the jets. The MAGMER would be deployed, powered, and controlled from a truck, to which it would be connected by hoses for water, compressed air, and collection of debris and by cables for electric power and communication (see Figure 1). The operation of the MAGMER on a typical large structure would necessitate the use of long cables and hoses, which can be heavy. To reduce the load of the hoses and cables on the MAGMER and thereby ensure its ability to adhere to vertical and overhanging surfaces, the hoses and cables would be paid out through telescopic booms that would be parts of a MAGMER support system.

The MAGMER would move by use of four motorized, steerable wheels, each of which would be mounted in an assembly that would include permanent magnets

Improvements in Fabrication of Sand/Binder Cores for Casting

Cores can be made stronger and more consistent.

Marshall Space Flight Center, Alabama

Three improvements have been devised for the cold-box process, which is a special molding process used to make sand/binder cores for casting hollow metal parts. These improvements are:

- The use of fiber-reinforced composite binder materials (in contradistinction to the non-fiber-reinforced binders used heretofore),
- The substitution of a directed-vortex core-blowing subprocess for a prior core-blowing process that involved a movable gassing plate, and
- The use of filters made from filtration-grade fabrics to prevent clogging of vents.

For reasons that exceed the scope of this article, most foundries have adopted the cold-box process for making cores for casting metals. However, this process is not widely known outside the metal-casting industry; therefore, a description of pertinent aspects of the cold-box process is prerequisite to a meaningful description of the aforementioned improvements.

In the cold-box process as practiced heretofore, sand is first mixed with a phenolic resin (considered to be part 1 of a three-part binder) and an isocyanate resin (part 2 of the binder). Then by use of compressed air, the mixture is blown into a core box, which is a mold for forming the core. Next, an amine gas (part 3 of the binder) that acts as a catalyst for polymerization of parts 1 and 2 is blown through the core box. Alternatively, a liquid amine that vaporizes during polymerization can be incorporated into the sand/resin mixture. Once polymerization is complete, the amine gas is purged from the core box by use of compressed air. The finished core is then removed from the core box.

The first-mentioned improvement is effected at the mixture-preparation stage by adding fibers to the mixture. In experiments, core specimens containing a variety of fibers were fabricated and subjected to tensile- and shear-strength tests. As shown in Figure 1, the strengths

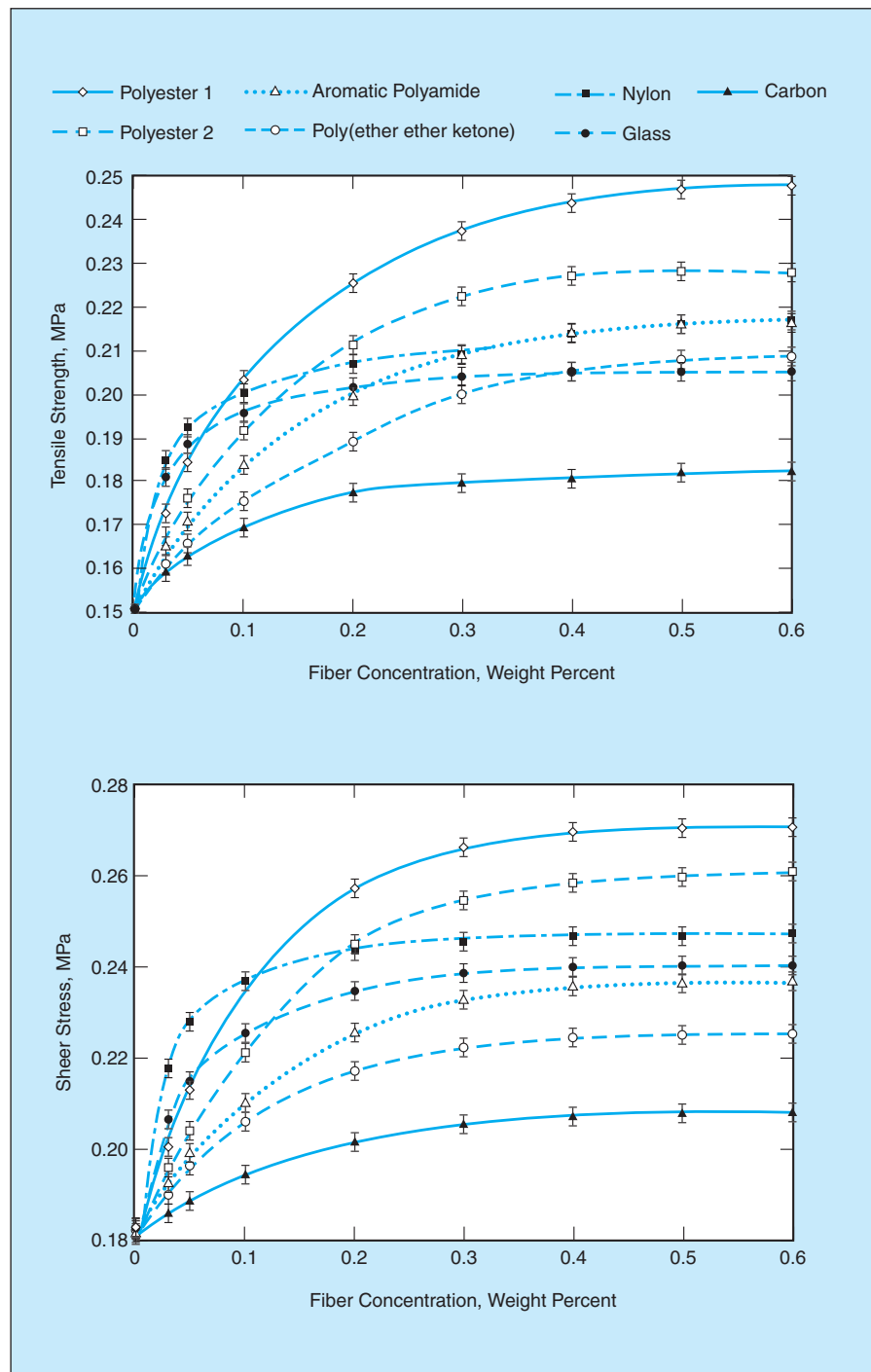


Figure 1. Tensile and Shear Strengths of core specimens were found to be increased by incorporation of a variety of fibers.

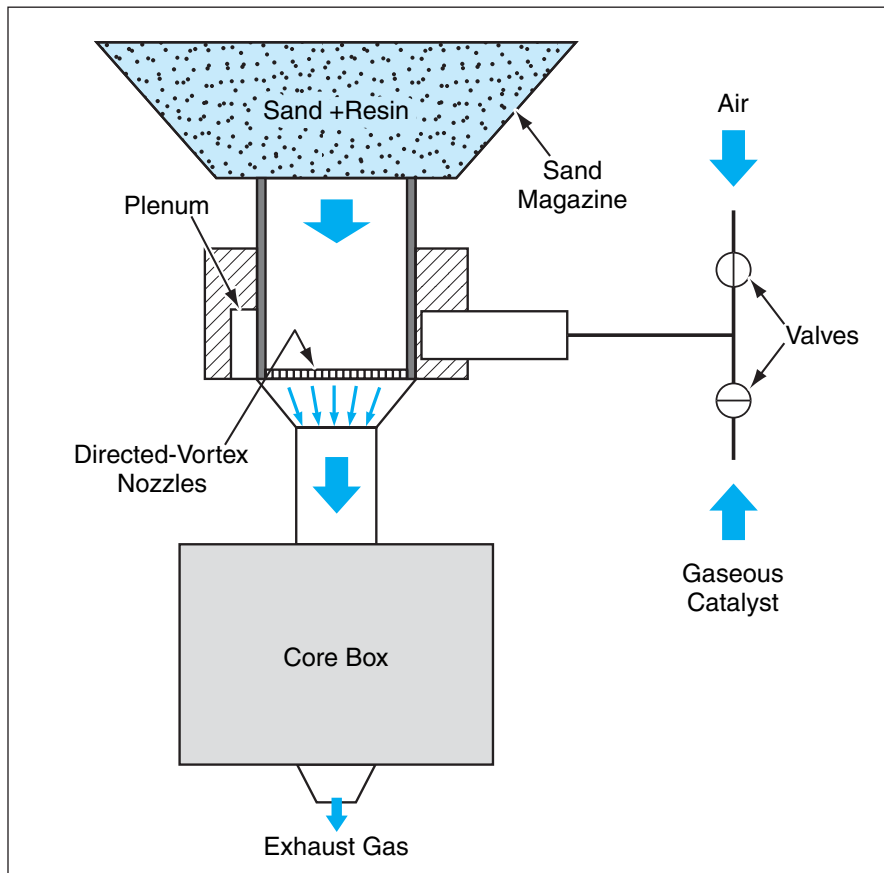


Figure 2. Air Flowing From Directed-Vortex Nozzles fluidizes the sand/resin mixture flowing into the core box.

of the specimens increased significantly with proportions of fibers up to about 0.3 weight percent.

The second-mentioned improvement — directed-vortex core-blowing — is directed toward obtaining more nearly optimum fluidization of the sand/resin mixture as the mixture is blown into the

core box. In this subprocess, the sand/resin mixture is fed from an overhead sand magazine, through an inlet blow tube, into the core box (see Figure 2). Compressed air is fed into an annular plenum, from whence it flows into the core box through a number of directed-vortex nozzles. The nozzles are designed

so that the flows from the nozzles generate a partial vacuum in the outlet from the sand magazine and pump a highly fluidized sand/resin mixture into the core box. Highly fluidized and accelerated sand particles travel long distances, the net result being more nearly complete and consistent filling of the core box. The directed-vortex nozzles are also used to feed in the amine gas for polymerization and the compressed air for purging the amine gas.

The third-mentioned improvement is directed toward preventing clogging of the exhaust vents of the core box. The total cross-sectional area of these vents should be about 80 percent of the cross-sectional area of the inlet blow tube — large enough for effective venting but just small enough to provide the back pressure needed to make the catalyst gas diffuse throughout the core to ensure a uniform cure. Vents are deliberately partially blocked by any of a variety of devices, typical ones being steel meshes or slotted steel disks. Heretofore it has been necessary to clean the vents at intervals during the process. By placing filters made of filtration-grade fabrics upstream of the vents, one prevents clogging of the vents, thereby eliminating the expense and loss of time associated with cleaning of the vents.

This work was done by Sayavur I. Bakhtiyarov, Ruel A. Overfelt, and Sabit Adanur of Auburn University for Marshall Space Flight Center. For further information, contact George Konstant, Auburn University Technology Transfer Associate Manager, (334) 844-4977 or ott@auburn.edu. MFS-31819/20/21

Solid Freeform Fabrication of Composite-Material Objects

Parts specified by CAD data files could be fabricated as needed.

Lyndon B. Johnson Space Center, Houston, Texas

Composite solid freeform fabrication (C-SFF) or composite layer manufacturing (CLM) is an automated process in which an advanced composite material (a matrix reinforced with continuous fibers) is formed into a freestanding, possibly complex, three-dimensional object. In CLM, there is no need for molds, dies, or other expensive tooling, and there is usually no need for machining to ensure that the object is formed to the desired net size and shape.

CLM is a variant of extrusion-type rapid prototyping, in which a model or prototype of a solid object is built up by controlled extrusion of a polymeric or other material through an orifice that is translated to form patterned layers. The second layer is deposited on top of the first layer, the third layer is deposited on top of the second layer, and so forth, until the stack of layers reaches the desired final thickness and shape.

The elements of CLM include (1) preparing a matrix resin in a form in

which it will solidify subsequently, (2) mixing the fibers and matrix material to form a continuous pre-impregnated tow (also called “towpreg”), and (3) dispensing the pre-impregnated tow from a nozzle onto a base while moving the nozzle to form the dispensed material into a patterned layer of controlled thickness. When the material deposited into a given layer has solidified, the material for the next layer is deposited and patterned similarly, and so forth, until the desired overall object has

been built up as a stack of patterned layers. Preferably, the deposition apparatus is controlled by a computer-aided design (CAD) system. The basic CLM concept can be adapted to the fabrication of parts from a variety of matrix materials.

It is conceivable that a CLM apparatus could be placed at a remote location on Earth or in outer space where (1) spare parts are expected to be needed but (2) it would be uneconomical or impractical to store a full inventory of spare parts. A

wide variety of towpregs could be prepared and stored on spools until needed. Long-shelf-life towpreg materials suitable for such use could include thermoplastic-coated carbon fibers and metal-coated SiC fibers. When a spare part was needed, the part could be fabricated by CLM under control by a CAD data file; thus, the part could be built automatically, at the scene, within hours or minutes.

This work was done by C. Jeff Wang and Jason Yang of Nanotek Instruments, Inc.,

and Bor Z. Jang of Auburn University for Johnson Space Center.

In accordance with Public Law 96-517, the contractor has elected to retain title to this invention. Inquiries concerning rights for its commercial use should be addressed to:

Nanotek Instruments, Inc.

1915 First Ave.

Opelika, AL 36801

Refer to MSC-22993, volume and number of this NASA Tech Briefs issue, and the page number.



Efficient Computational Model of Hysteresis

A useful approximate model applies to quasistatic displacements.

NASA's Jet Propulsion Laboratory, Pasadena, California

A recently developed mathematical model of the output (displacement) versus the input (applied voltage) of a piezoelectric transducer accounts for hysteresis. For the sake of computational speed, the model is kept simple by neglecting the dynamic behavior of the transducer. Hence, the model applies to static and quasistatic displacements only. A piezoelectric transducer of the type to which the model applies is used as an actuator in a computer-based control system to effect fine position adjustments. Because the response time of the rest of such a system is usually much greater than that of a piezoelectric transducer, the model remains an acceptably close approximation for the purpose of control computations, even though the dynamics are neglected.

The model (see Figure 1) represents an electrically parallel, mechanically series combination of backlash elements, each having a unique deadband width and output gain. The zeroth element in the parallel combination has zero deadband width and, hence, represents a linear component of the input/output relationship. The other elements, which have nonzero deadband widths, are used to model the nonlinear components of the hysteresis loop. The deadband widths and output gains of the elements are computed from experimental displacement-versus-voltage data. The hysteresis curve calculated by use of this model is piecewise linear beyond deadband limits.

Figure 2 presents a plot of the measured displacement of one piezoelectric transducer versus the applied potential. Overlaid on this plot is the piecewise-linear displacement-vs.-voltage curve computed by use of the model. In this case, the use of 13 parallel elements in the model was found sufficient to make the model approximate the experimental data within acceptably small error.

This work was done by Joel Shields of Caltech for NASA's Jet Propulsion Laboratory. Further information is contained in a TSP (see page 1). NPO-30546

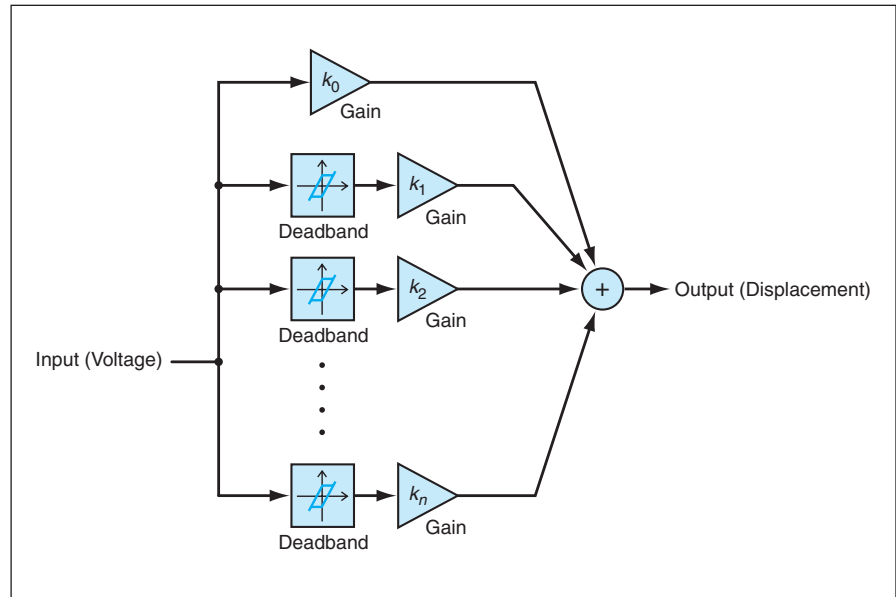


Figure 1. Backlash Elements comprising deadband and output-gain subelements are combined to construct a piecewise-linear mathematical model that approximates the nonlinear hysteretic response of a piezoelectric transducer.

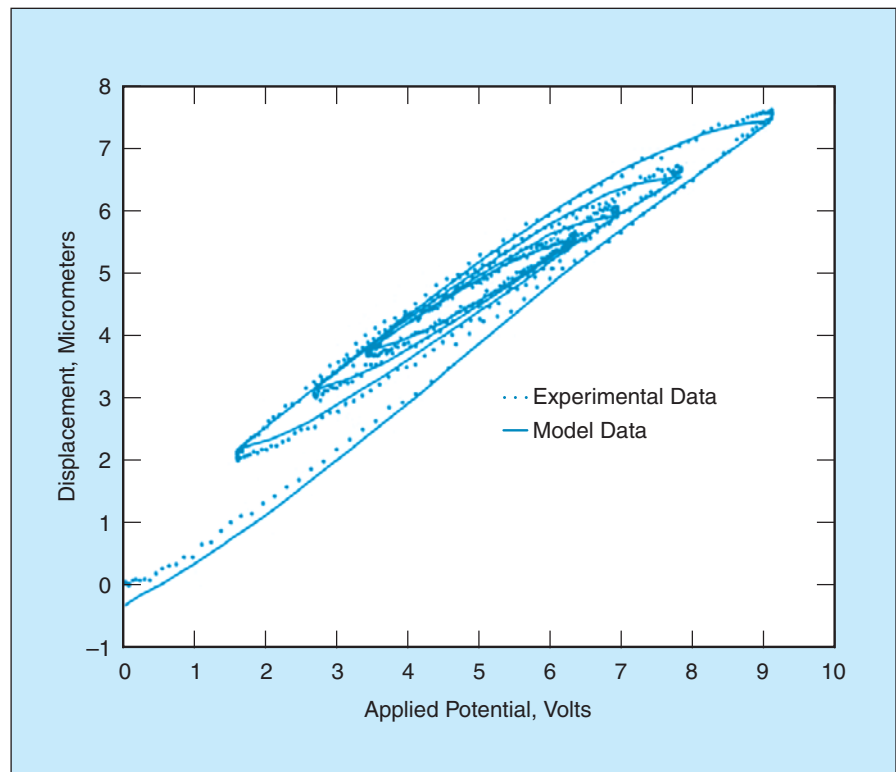


Figure 2. The Displacement of a Piezoelectric Transducer in response to an underdamped step voltage command was measured. It was also calculated by use of a model like that of Figure 1.

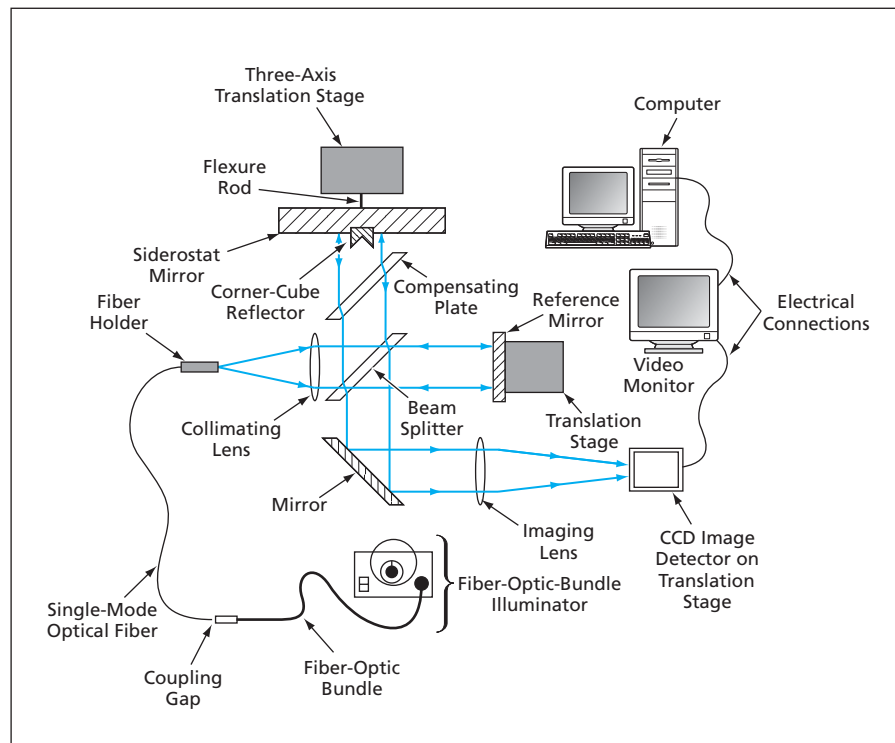
Gauges for Highly Precise Metrology of a Compound Mirror

High precision is achieved through careful attention to details of complex designs.

NASA's Jet Propulsion Laboratory, Pasadena, California

Three optical gauges have been developed for guiding the assembly and measuring precisely the reflecting surfaces of a compound mirror that comprises a corner-cube retroreflector glued in a hole on a flat mirror. In the specific application for which the gauges were developed, the compound mirror is part of a siderostat in a stellar interferometer. The flat-mirror portion of the compound mirror is the siderostat mirror; the retroreflector portion of the compound mirror is to be used, during operation of the interferometer, to monitor the location of the siderostat mirror surface relative to other optical surfaces of the interferometer. Nominally, the optical corner of the retroreflector should lie precisely on the siderostat mirror surface, but this precision cannot be achieved in fabrication: in practice, there remains some distance between the optical corner and the siderostat mirror surface. For proper operation of the interferometer, it is required to make this distance as small as possible and to know this distance within 1 nm. The three gauges make it possible to satisfy these requirements.

The first gauge is denoted the white-light assembly interferometer and is illustrated schematically in the figure. This is a Michelson type-interferometer with improvements over the basic Michelson design to make the attachment of the corner-cube retroreflector to the siderostat mirror as easy and accurate as possible. The initial alignment of the interferometer is performed soon after slow-curing glue has been applied to hold the corner-cube retroreflector in the siderostat mirror. For initial alignment of the interferometer, light is supplied by a laser diode; for subsequent observations, cool white light is supplied by a fiber-bundle illuminator. In either case, the supplied light is fed to the input end of a single-mode optical fiber, which, in turn, transmits a portion of the light to the input collimator of the interferometer. A reference mirror lies in one of the arms of the interferometer, while the siderostat and corner cube lie in the other arm. A digital micrometer on the reference-mirror translation stage is used only for calibration.



The **White-Light Assembly Interferometer** is one of three gauges designed specifically for use in aligning and measuring the alignment of the corner-cube retroreflector relative to the siderostat mirror to which it is bonded.

The output of the interferometer is reflected through a lens that images the siderostat-mirror/corner-cube assembly onto a monochrome charge-coupled device (CCD) image detector. The CCD output is digitized by a frame grabber and the digitized image data are processed in a personal computer running special-purpose software. After initial alignment of the interferometer, the interferometer is operated in a special high-tilt mode while the special-purpose software executes a very fast algorithm that analyzes the white-light interference fringes to locate the corner-cube and siderostat mirror surfaces relative to each other. If the measurement indicates excessive error, the corner cube can be removed or else its position adjusted before the glue sets hard. Experiments have shown that the use of the white-light assembly interferometer makes it possible to achieve a final optical corner/siderostat-mirror-surface distance of only about 50 nm, whereas heretofore, the final distance has typically been of the order of microns.

The second gauge, denoted the three-fiber gauge, is used to measure the devia-

tions from flatness of (1) nominally flat optical components that are used in the assembly of highly precise retroreflectors and (2) other nominally flat optical components used to measure the optical-corner/siderostat-mirror-surface distance to within 1 nm or less. The three-fiber gauge is based partly on the idea that the wave front emitted by a highly polished, single mode, polarization-maintaining optical fiber is nearly perfectly spherical, and when such wave fronts emitted by two perfectly matching fibers are interferometrically combined by a beam splitter at exactly equal distances from the tips of the fibers, the resulting fringe pattern can be used to deduce the deviation of the beam splitter from flatness.

In practice, the wave fronts from different fibers do not match perfectly, and this gives rise to complications that are addressed in the design and operation of the three-fiber gauge. The design and operation are extremely complex. The following are a few major features:

- The three-fiber gauge is so named because it utilizes laser wave fronts emitted by three optical fibers. (There

is also a fourth fiber, which is used for monitoring power.)

- Two of the fiber optical paths include delay lines containing electro-optical modulators.
- In operation, the modulators are used to create phase shifts that alter the interference fringes in ways that aid the extraction of the desired information.
- Images of the phase-shifted interference fringes are captured, digitized, and then analyzed by use of a very robust fringe-tracking and phase-unwrapping algorithm developed specifically for this gauge.
- The final product of the analysis is a map, accurate to 1 nm or less, of the deviation from flatness of the component under test.

The third gauge is denoted the split-fiber-beam, single-fiber interferometer. This gauge utilizes a reference optical flat that has been calibrated by use of the three-fiber gauge for measuring the optical-corner/siderostat-mirror-surface distance. A single laser beam is delivered by an optical fiber, and is split in half and collimated by two off-axis paraboloidal reflectors. The collimated first half beam is aimed at the siderostat/retroreflector assembly. The light reflected from the assembly is sent back toward the fiber by the same paraboloid that collimated it. This light is then reflected from the tip of the optical fiber and interferes with the second half beam coming out of the fiber. The resulting two divergent beams are inter-

cepted and collimated by the second paraboloidal reflector, then focused by a third paraboloidal reflector onto an image detector for analysis of interference fringes. For the purpose of shifting phases in order to shift interference fringes to aid the extraction of the required information, the siderostat/retroreflector assembly is mounted on a closed-loop, three-axis piezoelectric transducer that moves the assembly in controlled steps that can be resolved to 1 nm.

This work was done by Yekta Gursel of Caltech for NASA's Jet Propulsion Laboratory. Further information is contained in a TSP (see page 1). NPO-30804

Improved Electrolytic Hydrogen Peroxide Generator

Energy efficiency exceeds that of a prior electrolytic H₂O₂ generator.

Lyndon B. Johnson Space Center, Houston, Texas

An improved apparatus for the electrolytic generation of hydrogen peroxide dissolved in water has been developed. The apparatus is a prototype of H₂O₂ generators for the safe and effective sterilization of water, sterilization of equipment in contact with water, and other applications in which there is need for hydrogen peroxide at low concentration as an oxidant. Potential applications for electrolytic H₂O₂ generators include purification of water for drinking and for use in industrial processes, sanitation for hospitals and biotechnological industries, inhibition and removal of biofouling in heat exchangers, cooling towers, filtration units, and the treatment of wastewater by use of advanced oxidation processes that are promoted by H₂O₂.

The apparatus is an electrochemical cell in which the electrodes are located on opposite sides of a commercially available polymeric membrane, which separates the electrolytes of the two electrolytic half-reactions. One of the half-cells produces the biocidal aqueous H₂O₂ product; the product of the other half-cell restores the biocidal solution to potability. The apparatus is designed to process water that is neutral (in the sense of neither acidic nor alkaline) or nearly neutral, to consume minimal energy, and to operate without need to supply nonregenerable material(s) other than the small proportion of water that is electrolyzed.

The energy efficiency of the cell is increased through improved microscopic mixing of the electrolytes near

the electrodes without need for large bulk electrolyte flow rates: this is accomplished by rotating the electrodes relative to the rest of the cell (in contradistinction to forcing electrolyte flow over stationary electrodes). Even though the design of this prototype cell is unoptimized, the total energy consumption per unit of product was found to be 60 percent less than that of a common planar H₂O₂-generating cell in operation at similar Faradaic and production rates.

This work was done by Patrick I. James of Eltron Research, Inc., for Johnson Space Center. For further information, contact the Johnson Innovative Partnerships Office at (281) 483-3809. MSC-23093

High-Power Fiber Lasers Using Photonic Band Gap Materials

PBG materials would be exploited to increase power levels and efficiencies.

NASA's Jet Propulsion Laboratory, Pasadena, California

High-power fiber lasers (HPFLs) would be made from photonic band gap (PBG) materials, according to the proposal. Such lasers would be scalable in the sense that a large number of fiber lasers could be arranged in an array or bundle and then operated in phase-locked condition

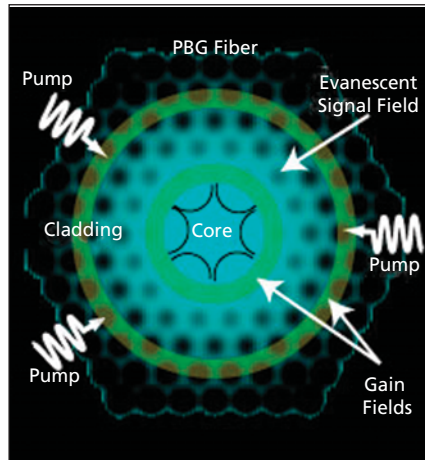
to generate a superposition and highly directed high-power laser beam. It has been estimated that an average power level as high as 1,000 W per fiber could be achieved in such an array.

Examples of potential applications for the proposed single-fiber lasers include

welding and laser surgery. Additionally, the bundled fibers have applications in beaming power through free space for autonomous vehicles, laser weapons, free-space communications, and inducing photochemical reactions in large-scale industrial processes.

The proposal has been inspired in part by recent improvements in the capabilities of single-mode fiber amplifiers and lasers to produce continuous high-power radiation. In particular, it has been found that the average output power of a single strand of a fiber laser can be increased by suitably changing the doping profile of active ions in its gain medium to optimize the spatial overlap of the electromagnetic field with the distribution of active ions. Such optimization minimizes pump power losses and increases the gain in the fiber laser system. The proposal would expand the basic concept of this type of optimization to incorporate exploitation of the properties (including, in some cases, nonlinearities) of PBG materials to obtain power levels and efficiencies higher than are now possible. Another element of the proposal is to enable pumping by concentrated sunlight.

Somewhat more specifically, the proposal calls for exploitation of the properties of PBG materials to overcome a number of stubborn adverse phenomena that have impeded prior efforts to perfect HPFLs. The most relevant of those phenomena is amplified spontaneous emission (ASE), which causes saturation of gain and power at undesirably low levels, and scattering of light from dopants. In designing a given fiber laser for reduced ASE, care must be taken to maintain a correct fiber structure for eventual scaling to an array of



In this Image Generated in a Simulation of a PBG fiber laser, the intensity of a single-mode signal decaying away from the waveguide core is represented by the intensity of the bright field against the dark fiber holes. Also shown here are different gain regions, which would be exposed to different evanescent fields by virtue of a band-gap shift, which would depend on the intensity of radiation in the core. The band-gap shift would be exploited as a feedback control mechanism.

many such lasers such that the interactions among all the members of the array would cause them to operate in phase lock. Hence, the problems associated with improving a single-fiber laser are not entirely separate from the bundling problem, and some designs for individual fiber lasers may be better than others if the fibers are to be incorporated into bundles.

Extensive calculations, expected to take about a year, must be performed

in order to determine design parameters before construction of prototype individual and fiber lasers can begin. The design effort can be expected to include calculations to optimize overlaps between the electromagnetic modes and the gain media and calculations of responses of PBG materials to electromagnetic fields. Design alternatives and physical responses that may be considered include simple PBG fibers with no intensity-dependent responses, PBG fibers with intensity-dependent band-gap shifting (see figure), and broad-band pumping made possible by use of candidate broad-band pumping media in place of the air or vacuum gaps used in prior PBG fibers.

This work was done by Leo DiDomenico and Jonathan Dowling of Caltech for NASA's Jet Propulsion Laboratory. Further information is contained in a TSP (see page 1).

In accordance with Public Law 96-517, the contractor has elected to retain title to this invention. Inquiries concerning rights for its commercial use should be addressed to:

*Innovative Technology Assets Management
JPL*

*Mail Stop 202-233
4800 Oak Grove Drive
Pasadena, CA 91109-8099
(818) 354-2240*

E-mail: iaoffice@jpl.nasa.gov

Refer to NPO-40552, volume and number of this NASA Tech Briefs issue, and the page number.

Ontology-Driven Information Integration

Models developed in different domains of expertise can be automatically integrated.

Lyndon B. Johnson Space Center, Houston, Texas

Ontology-driven information integration (ODII) is a method of computerized, automated sharing of information among specialists who have expertise in different domains and who are members of subdivisions of a large, complex enterprise (e.g., an engineering project, a government agency, or a business). In ODII, one uses rigorous mathematical techniques to develop computational models of engineering and/or business information and processes. These models are then used to develop software tools that support the reliable processing and exchange of information among the subdivisions of this enterprise or between this enterprise and other enterprises.

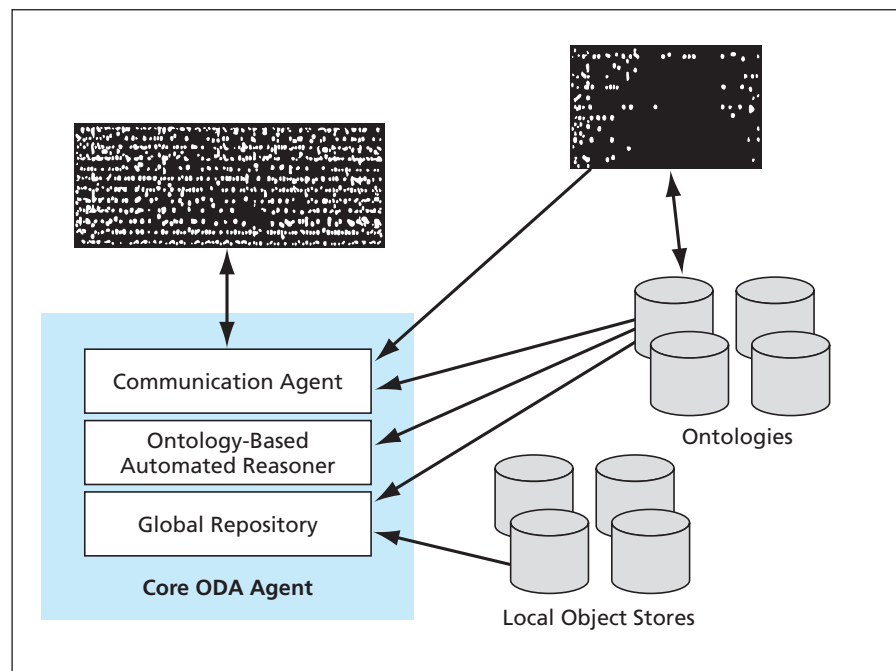
The need for ODII arises because in the absence of an automated means of integrating information, enterprises and subdivisions of enterprises tend to become somewhat isolated from each other, making the overall enterprises less efficient than they could otherwise be. The information generated in various domains of knowledge in organizational subdivisions is typically stored in the form of models. Consequently, to a large degree, the information-integration problem reduces to a problem of integration of models. The primary source of the model-integration problem is the fact that the experts in each different domain use a different modeling method with its own syntax for constructing models and its own semantics for interpreting the constructions. (This combination of syntax and semantics, together with any other explicit and/or implicit background information specific to the domain, is denoted loosely as the “ontology” of the domain for the purposes of ODII.) Hence, to move information from models in one domain to those in another domain, it is necessary to use a human or computer “translator.” Of course, translation by humans would be too inefficient to enable integration of models in real time. ODII was conceived to provide real-time computer translation.

ODII is best summarized in terms of some of the concepts and constructs

that have been formalized at various stages of its development. The construct of one of the earlier stages is an ontology-driven information-integration architecture (ODA) based on the concept of an agent (the core ODA agent) that performs the information-integration functions. As depicted schematically in the figure, the core ODA agent

and it enables the core ODA agent to propagate those implications to the relevant experts in the various domains.

The ontology-based automated reasoner is responsible for detecting conflicts, propagating changes, and maintaining consistency in the global repository. It is also responsible for notifying the communication agent of new



The ODA is a conceptual architecture for implementation of ODII.

comprises a communication agent, an ontology-based automated reasoner, and a global repository.

The communication agent is responsible for enabling the integration of modeling software tools in the computational environment and transferring information from and to those tools that have been integrated. It receives information from integrated tools and communicates the information to the global repository for storage and to the automated reasoner for propagation of changes and maintenance of consistency. Thus, it keeps the core ODA apprised of the information generated within each domain and, hence, enables the core ODA agent to determine the implications of that information in all relevant contexts;

information that has been deduced so that this information can be propagated back to the various experts working on the given project. It uses the constraints defined in the ontology library to perform its function. It thus keeps the core ODA agent aware of all the constraints that connect the objects and activities in the various domains.

The global repository is responsible for storing, updating, and retrieving information available about a project. It receives updated information from the communication agent and from the automated reasoner. The information contained in the global repository can be browsed and edited through a graphical user interface. Even though the global repository is conceptually

considered one knowledge base, the information can be physically stored in networked databases (represented by the local object stores in the figure). The ontologies of the domains relevant to the enterprise at hand are considered part of the global repository. Hence, the global repository provides the necessary background knowledge for all relevant domains.

Other ODII developments to date include the following:

- The ODA has been implemented in a software system called the Integrated Design System Environment (IDSE).
- An ODA subarchitecture denoted the design rationale management (DRM)

framework has been devised as a means to capture information on the reasons for design choices. This information is needed in ODII because failure to understand design rationale severely limits reuse of design information and makes it difficult to determine whether proposed design modifications are acceptable.

- A prototype program called the Ontology Capture and Browsing Tool (OCBT) has been incorporated into IDSE. OCBT provides support for capturing and browsing ontologies through a user-friendly graphical interface. A commercial version of OCBT, called IDEF5, was under devel-

opment at the time of reporting the information for this article.

- Also under development at the time of reporting was the Generic Application Framework (GAPP) computer program, which is intended to provide integration among models developed in different domains and to display all models within a single computational environment.

This work was done by Florence Tissot and Chris Menzel of Knowledge Based Systems, Inc., for Johnson Space Center. For further information, contact the Johnson Innovative Partnerships Office at (281) 483-3809. MSC-22933



Quantifying Traversability of Terrain for a Mobile Robot

A document presents an updated discussion on a method of autonomous navigation for a robotic vehicle navigating across rough terrain. The method at an earlier stage of development was described in "Navigating a Mobile Robot Across Terrain Using Fuzzy Logic" (NPO-21199), *NASA Tech Briefs*, Vol. 27, No. 2 (February 2003), page 5a. To recapitulate: The method involves, among other things, the use of a measure of traversability, denoted the fuzzy traversability index, which embodies the information about the slope and roughness of terrain obtained from analysis of images acquired by cameras mounted on the robot. The improvements presented in the report focus on the use of the fuzzy traversability index to generate a traversability map and a grid map for planning the safest path for the robot. Once grid traversability values have been computed, they are utilized for rejecting unsafe path segments and for computing a traversal-cost function for ranking candidate paths, selected by a search algorithm, from a specified initial position to a specified final position. The output of the algorithm is a set of waypoints designating a path having a minimal-traversal cost.

This work was done by Ayanna Howard, Homayoun Seraji, and Barry Werger of Caltech for NASA's Jet Propulsion Laboratory.

The software used in this innovation is available for commercial licensing. Please contact Karina Edmonds of the California Institute of Technology at (818) 393-2827. Refer to NPO-30744.

More About Arc-Welding Process for Making Carbon Nanotubes

A report presents additional information about the process reported in "Manufacturing High-Quality Carbon Nanotubes at Lower Cost" (GSC-14601) *NASA Tech Briefs*, Vol. 28, No. 9 (September 2004), page 62. To recapitulate: High-quality batches of carbon nanotubes are produced at relatively low cost in a modified atmospheric-pressure electric-arc welding process that does

not include the use of metal catalysts. What would normally be a welding rod and a weldment are replaced by an amorphous carbon anode rod and a wider, hollow graphite cathode rod. Both electrodes are water-cooled. The cathode is immersed in ice water to about 0.5 cm from the surface. The system is shielded from air by flowing helium during arcing. As the anode is consumed during arcing at 20 to 25 A, it is lowered to maintain it at an approximately constant distance above the cathode. The process causes carbon nanotubes to form on the lowest 5 cm of the anode. The arcing process is continued until the anode has been lowered to a specified height. The nanotube-containing material is then harvested. The additional information contained in the instant report consists mostly of illustrations of carbon nanotubes and a schematic diagram of the arc-welding setup, as modified for the production of carbon nanotubes.

This work was done by Jeanette M. Benavides and Henning Leidecker of Goddard Space Flight Center. Further information is contained in a TSP (see page 1).

This invention is owned by NASA, and a patent application has been filed. Inquiries concerning nonexclusive or exclusive license for its commercial development should be addressed to the Patent Counsel, Goddard Space Flight Center; (301) 286-7351. Refer to GSC-14435.

Controlling Laser Spot Size in Outer Space

Three documents discuss a method of controlling the diameter of a laser beam projected from Earth to any altitude ranging from low orbit around the Earth to geosynchronous orbit. Such laser beams are under consideration as means of supplying power to orbiting spacecraft at levels of the order of tens of kilowatts apiece. Each such beam would be projected by use of a special-purpose telescope having an aperture diameter of 15 m or more. Expanding the laser beam to such a large diameter at low altitude would prevent air breakdown and render the laser beam eye-safe. Typically, the telescope would include an adaptive-optics concave primary mirror and a convex secondary mirror. The laser beam transmitted out to the satellite would remain in the near

field on the telescope side of the beam waist, so that the telescope focal point would remain effective in controlling the beam width. By use of positioning stages having submicron resolution and repeatability, the relative positions of the primary and secondary mirrors would be adjusted to change the nominal telescope object and image distances to obtain the desired beam diameter (typically about 6 m) at the altitude of the satellite. The limiting distance D_L at which a constant beam diameter can be maintained is determined by the focal range of the telescope $4\lambda f^2$ where λ is the wavelength and f the f /number of the primary mirror. The shorter the wavelength and the faster the mirror, the longer D_L becomes.

This work was done by Harold E. Bennett of Bennett Optical Research, Inc., for Marshall Space Flight Center.

In accordance with Public Law 96-517, the contractor has elected to retain title to this invention. Inquiries concerning rights for its commercial use should be addressed to:

*Dr. Harold Bennett, President
Bennett Optical Research, Inc.
916 N. Randall Street
Ridgecrest, CA 93555*

*E-mail: Bennett@bennettopticalresearch.com
Refer to MFS-32039-1, volume and number of this NASA Tech Briefs issue, and the page number.*

Software-Reconfigurable Processors for Spacecraft

A report presents an overview of an architecture for a software-reconfigurable network data processor for a spacecraft engaged in scientific exploration. When executed on suitable electronic hardware, the software performs the functions of a physical layer (in effect, acts as a software radio in that it performs modulation, demodulation, pulse-shaping, error correction, coding, and decoding), a data-link layer, a network layer, a transport layer, and application-layer processing of scientific data. The software-reconfigurable network processor is undergoing development to enable rapid prototyping and rapid implementation of communication, navigation, and scientific signal-processing functions; to provide a long-lived communication infrastructure; and to provide greatly improved scientific-instrumentation and

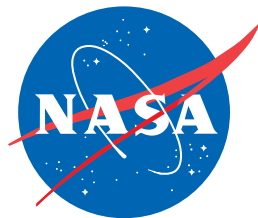
scientific-data-processing functions by enabling science-driven in-flight reconfiguration of computing resources devoted to these functions. This development is an extension of terrestrial radio and network developments (e.g., in the cellular-telephone industry) implemented in software running on such

hardware as field-programmable gate arrays, digital signal processors, traditional digital circuits, and mixed-signal application-specific integrated circuits (ASICs).

This work was done by Allen Farrington, Andrew Gray, Bryan Bell, Valerie Stanton, Yong Chong, Kenneth Peters, Clement Lee,

and Jeffrey Srinivasan of Caltech for NASA's Jet Propulsion Laboratory. Further information is contained in a TSP (see page 1).

This software is available for commercial licensing. Please contact Karina Edmonds of the California Institute of Technology at (818) 393-2827. Refer to NPO-30357.



National Aeronautics and
Space Administration